

# CONVERGENCE ANALYSIS OF CONTRAST SOURCE INVERSION TYPE METHODS FOR ACOUSTIC INVERSE MEDIUM SCATTERING PROBLEMS

QIAO HU\*, BO ZHANG†, AND HAIWEN ZHANG‡

**Abstract.** The contrast source inversion (CSI) method and the subspace-based optimization method (SOM) are first proposed in 1997 and 2009, respectively, and subsequently modified. The two methods and their variants share several properties and thus are called the CSI-type methods. The CSI-type methods are efficient and popular methods for solving inverse medium scattering problems, but their rigorous convergence remains an open problem. In this paper, we propose two iteratively regularized CSI-type (IRCSI-type) methods with a novel  $\ell_1$  proximal term as the iteratively regularized term: the iteratively regularized CSI (IRCSI) method and the iteratively regularized SOM (IR-SOM) method, which have a similar computation complexity to the original CSI and SOM methods, respectively, and prove their global convergence under natural and weak conditions on the original objective function. To the best of our knowledge, this is the first convergence result for iterative methods of solving nonlinear inverse scattering problems with a fixed frequency. The convergence and performance of the two IRCSI-type algorithms are illustrated by numerical experiments.

**Key words.** Inverse medium scattering, CSI method, SOM method, Iteratively regularized methods, Convergence analysis

**1. Introduction.** This paper is concerned with the inverse problem of scattering of time-harmonic acoustic plane waves by an inhomogeneous medium. Such a problem has wide and important applications in many areas such as geophysical exploration, nondestructive testing, and medical imaging.

The inverse medium scattering problem consists in recovering the refractive index of an inhomogeneous medium (or, equivalently, the contrast function of the refractive index of the inhomogeneous medium) from the near-field or far-field measurement data. Consequently, the inverse medium scattering problem can be formulated as the following nonlinear operator equation

$$(1.1) \quad F(x) = y,$$

where  $F$  denotes the nonlinear forward operator and  $x$  and  $y$  denote the unknown refractive index of the inhomogeneous medium (or its contrast) and the measurement data, respectively. The reader is referred to the monographs [17, 21] for a comprehensive discussion on the mathematical and computational aspects of inverse medium scattering problems and other types of inverse scattering problems.

Many iterative regularization methods have been developed for solving inverse medium scattering problems based on the operator equation (1.1) and the Fréchet derivative (or the Fréchet conjugate derivative) of the forward operator  $F$ ; see, e.g., the Newton–Kantorovich method [45] for the electromagnetic wave case, the recursive linearization method with respect to the frequency for the case of multi-frequency measurements or with respect to the spatial frequency for the case of fixed frequency

---

\*NCMIS and Academy of Mathematics and Systems Science, Chinese Academy of Sciences, Beijing 100190, China and School of Mathematical Sciences, University of Chinese Academy of Sciences, Beijing 100049, China ([huqiao2020@amss.ac.cn](mailto:huqiao2020@amss.ac.cn)).

†SKLMS and Academy of Mathematics and Systems Science, Chinese Academy of Sciences, Beijing 100190, China and School of Mathematical Sciences, University of Chinese Academy of Sciences, Beijing 100049, China ([b.zhang@amt.ac.cn](mailto:b.zhang@amt.ac.cn)).

‡SKLMS and Academy of Mathematics and Systems Science, Chinese Academy of Sciences, Beijing 100190, China ([zhanghaiwen@amss.ac.cn](mailto:zhanghaiwen@amss.ac.cn)).

measurements [3, 4, 5, 6, 7, 8, 18, 60], the preconditioned Newton method [28, 29, 30, 38] and the iteratively regularized Gauss–Newton method (IRGNM) with a learned projector [41]. Note that these iterative methods need to solve the forward scattering problem repeatedly in order to compute the Fréchet derivative of the forward operator and thus are computationally expensive.

To avoid the computations of the Fréchet derivative of the forward operator, much effort has been made for developing efficient iterative methods for inverse medium scattering problems; see, e.g., the Born iterative method (BIM) [58], the distorted-Born iterative method (DBIM) [19, 44, 59], the contrast source inversion (CSI) method [53, 54, 55] and the subspace-based optimization method (SOM) [14, 15, 16]. In particular, the original CSI method was first proposed by van den Berg and Kleinman in 1997 [53]. The main idea of the CSI method is to reformulate the inverse medium scattering problem (1.1) into an optimization problem which is then solved by alternatively updating the contrast and the contrast source. The SOM method was first proposed by Chen in 2009 [14] to accelerate the CSI method and subsequently further improved [15, 16]. The main idea of the SOM method is to use the singular value decomposition (SVD) to reduce the computation time when updating the contrast source. As shown in Sections 3 and 4, the CSI and SOM methods are very similar in structure and can be reformulated in the following general framework

$$(1.2) \quad \arg \min_{(x,y) \in \mathbb{C}^{n_1+\dots+n_J} \times \mathbb{C}^m} \Psi(x,y) = \sum_{j=1}^J \Psi_j(x_j, y).$$

Therefore, for convenience, the CSI and SOM methods are called the CSI-type method in this paper. Due to the easy implementation and low computational cost of the CSI-type methods, they are widely used in the area of electromagnetic inversion and imaging and in applications (see, e.g., [40, 42, 43, 46, 49, 57, 62] and the monographs [17, 56]). However, their convergence property has not been established yet.

We now comment on the convergence property of the iterative methods for nonlinear inverse scattering problems. In [9], under some reasonable assumptions on the forward operator  $F$  in (1.1), Bao and Triki established convergence with error estimates of the recursive linearization method for solving inverse medium scattering problems with multi-frequency measurements; by using this result, they proved in [9] the first convergence result along with the error estimate for the recursive linearization method of Chen [18]. The convergence of the recursive linearization method has also been proved in [47, 48] for the inverse acoustic obstacle scattering problem with multi-frequency measurements in the sound-soft obstacle case. Convergence of iterative methods has been studied extensively for general nonlinear ill-posed problems with the form (1.1) under some source conditions and nonlinear conditions on the operator  $F$ ; see, e.g., [2, 10, 31, 36, 39] for the iteratively regularized Gauss–Newton method (IRGNM), [24] for the Levenberg–Marquardt (LM) method, [25] for the Newton–CG method and [26] for the Landweber iteration method; see also the survey paper [12] and the monograph [37] for a comprehensive discussion on the source conditions and nonlinear conditions on  $F$ . However, for the case of nonlinear inverse medium and obstacle scattering problems at a fixed frequency, although some progress has been made through the work of Hohage [31, 32, 34, 35] and others on logarithmic or variational source conditions in the convergence analysis of Newton-type methods for the operator  $F$ , the nonlinear conditions on the forward operator  $F$  needed for the general convergence results could not be verified yet (see, e.g., [27] for the Landweber iteration method for inverse obstacle scattering, [31, 32, 33] for Newton-type meth-

ods for inverse obstacle scattering and [28, 34, 35] for IRGNM for inverse medium scattering). Therefore, to the best of our knowledge, no convergence result has been established for Newton-type methods in nonlinear inverse scattering problems with single-frequency measurements (see also the survey paper [20, pp. 788; Open Problem 3, pp. 802]).

In this paper, we propose iteratively regularized CSI (IRCSI) and iteratively regularized SOM (IRSOM) methods, called IRCSI-type methods, for solving the inverse medium scattering problem, based on the general framework (1.2) and prove their global convergence under very weak and natural conditions on the objective function  $\Psi$  (see Assumption 5.2 below). Efficient iterative methods have been developed for solving the optimization problem of the form (1.2), such as the Block Coordinate Descent (BCD) method [50], the Proximal Alternating Minimization (PAM) method [1] and the Proximal Alternating Linearized Minimization (PALM) method [11]. However, the convergence of these iterative methods can not be guaranteed unless the Kurdyka-Łojasiewicz (KL) property holds for the objective function  $\Psi$  [1, 11, 13]. In order to overcome this difficulty, our IRCSI-type methods employ a novel  $\ell_1$  proximal term as the iteratively regularized term, ensuring the global convergence of the iteration sequence generated by the IRCSI-type methods (see Theorem 5.4 below). Further, it is proved that the limit point of the iteration sequence of the IRCSI-type methods is an  $\varepsilon$ -stationary point of the original objective function  $\Psi$ , where  $\varepsilon$  is a very small constant defined in terms of the regularization parameters (see (5.5) in Theorem 5.4 below). As corollaries of the general convergence Theorem 5.4, the convergence of the iterative sequences generated by the IRCSI and IRSOM methods follows easily (see Corollaries 5.5 and 5.6 below). As far as we know, this is the first convergence result for iterative methods for solving nonlinear inverse medium or obstacle scattering problems with single-frequency measurement data. As demonstrated the algorithmic formulations in Sections 3 and 4 and the numerical experiments in Section 6, our IRCSI-type methods have a similar computation complexity to the corresponding original CSI-type methods. Further, the numerical results presented in Section 6 show that our IRCSI-type methods outperform the corresponding original CSI-type methods in stability and convergence. In fact, from the numerical experiments it seems that, in the case with noisy measurement data, the original CSI-type methods may not converge, whilst our IRCSI-type methods converge.

The remaining part of the paper is organized as follows. In Section 2, we introduce the direct and inverse medium scattering problems. Section 3 presents the original CSI and SOM methods for solving the inverse scattering problem. The IRCSI and IRSOM algorithms are proposed in Section 4, and their convergence is proved in Section 5. Numerical experiments are carried out in Section 6 to compare the performance of the IRCSI-type methods with the original CSI-type methods. Conclusions are given in Section 7.

**2. The direct and inverse medium scattering problems.** In this section, we describe the direct and inverse scattering problems for time-harmonic acoustic wave propagation in an inhomogeneous medium in  $\mathbb{R}^n$  ( $n = 2, 3$ ). Assume that the inhomogeneous medium is characterized by a piecewise smooth complex refractive index  $b(x)$  with the contrast  $m(x) := b(x) - 1$  having a compact support in  $\mathbb{R}^n$ . The direct problem is to find the total field  $u(x)$ , given a wave number  $\kappa > 0$  and an incident wave  $u^i(x)$  (in this paper we consider the incident plane wave  $u^i(x) = e^{i\kappa x \cdot d}$  with  $d$  being the incident direction in  $\mathbb{S}^{n-1} := \{x \in \mathbb{R}^n : |x| = 1\}$ ). The total field  $u(x) := u^i(x) + u^s(x)$ , which is the sum of the incident field  $u^i(x)$  and the scattered

field  $u^s(x)$ , satisfies the following scattering problem

$$(2.1) \quad \Delta u + \kappa^2 b(x)u = 0 \quad \text{in } \mathbb{R}^n,$$

$$(2.2) \quad \lim_{|x| \rightarrow \infty} |x|^{\frac{n-1}{2}} \left( \frac{\partial u^s}{\partial |x|} - i\kappa u^s \right) = 0 \quad \text{uniformly in all directions } \hat{x} := \frac{x}{|x|}.$$

Here, (2.1) is called the reduced wave equation which is reduced to the Helmholtz equation in the case  $b(x) \equiv 1$ , and (2.2) is called the Sommerfeld radiation condition.

The existence of a unique solution to the scattering problem (2.1)–(2.2) can be established by using its equivalent Lippmann–Schwinger integral equation (see, e.g., [21, Section 8.2] and [52]):

$$(2.3) \quad u(x) = u^i(x) + \kappa^n \int_{\mathbb{R}^n} \Phi(\kappa|x-y|)m(y)u(y)dy, \quad x \in \mathbb{R}^n.$$

Here,  $\Phi(\kappa r)$  is given by

$$\Phi(\kappa r) = \begin{cases} \frac{i}{4} H_0^{(1)}(\kappa r), & n = 2, \\ \frac{1}{4\pi} \frac{e^{i\kappa r}}{\kappa r}, & n = 3, \end{cases}$$

where  $H_0^{(1)}$  is the Hankel function of the first kind of order zero. It was proved in [21, Section 8.2] that the Lippmann–Schwinger integral equation (2.3) is uniquely solvable and

$$(2.4) \quad u = [I - \mathcal{T}_{\kappa, m}]^{-1} u^i,$$

where the integral operator  $\mathcal{T}_{\kappa, m} : C(\bar{B}) \rightarrow C(\bar{B})$ , with  $B$  being a bounded open ball containing the support of  $m(x)$ , is defined by

$$(\mathcal{T}_{\kappa, m}v)(x) := \kappa^n \int_{\mathbb{R}^n} \Phi(\kappa|x-y|)m(y)v(y)dy, \quad x \in \bar{B},$$

and  $I - \mathcal{T}_{\kappa, m} : C(\bar{B}) \rightarrow C(\bar{B})$  is bijective and has a bounded inverse.

The scattered field  $u^s(x)$  has the following far-field asymptotic behavior

$$u^s(x) = \frac{e^{i\kappa|x|}}{|x|^{(n-1)/2}} \left\{ u^\infty(\hat{x}) + \mathcal{O}\left(\frac{1}{|x|}\right) \right\}, \quad |x| \rightarrow \infty,$$

where  $\hat{x} := x/|x| \in \mathbb{S}^{n-1}$  denotes the unit vector in the direction of  $x$ . This, together with (2.3) and the asymptotic behavior at the infinity of  $\Phi(\kappa|x-y|)$  (see, e.g., [21, (2.15) and (3.105)]), implies that the far-field pattern  $u^\infty(\hat{x})$  is given by

$$(2.5) \quad u^\infty(\hat{x}) = \theta_{n, \kappa} \int_{\mathbb{R}^n} e^{-i\kappa\hat{x}\cdot y} m(y)u(y)dy, \quad \theta_{n, \kappa} = \begin{cases} \frac{\kappa^2 e^{i\frac{\pi}{4}}}{\sqrt{8\kappa\pi}}, & n = 2, \\ \frac{\kappa^2}{4\pi}, & n = 3. \end{cases}$$

From this representation and (2.4), it is easy to see that the far-field pattern  $u^\infty(\hat{x})$  depends on the contrast  $m(x)$  nonlinearly.

Making use of a number of incident plane waves  $u_j^i(x) = e^{i\kappa x \cdot d_j}$  with different incident directions  $d_j$ ,  $j = 1, \dots, J$ , we have

$$(2.6) \quad u_j(x) = u_j^i(x) + \kappa^n \int_{\mathbb{R}^n} \Phi(\kappa|x-y|)m(y)u_j(y)dy,$$

$$(2.7) \quad u_j^\infty(\hat{x}) = \theta_{n,\kappa} \int_{\mathbb{R}^n} e^{-i\kappa\hat{x}\cdot y}m(y)u_j(y)dy$$

with  $j = 1, \dots, J$ . These equations are called the state and data equations, respectively.

**Inverse problem:** The inverse medium scattering problem is to determine the unknown contrast  $m(x)$  from the given measurement data  $u_j^\infty(\hat{x})$ ,  $j = 1, \dots, J$ .

In (2.6) and (2.7), both the total field  $u_j(x)$  and the contrast  $m(x)$  are unknown. For each  $j$ , define the product  $m(x)u_j(x)$  as a single quantity  $\omega_j(x)$ , which is referred to as the contrast source:

$$\omega_j(x) := m(x)u_j(x).$$

By multiplying both sides of the equation (2.6) with  $m(x)$ , the state equation becomes

$$(2.8) \quad \omega_j(x) = m(x)u_j^i(x) + m(x)\kappa^n \int_{\mathbb{R}^n} \Phi(\kappa|x-y|)\omega_j(y)dy, \quad j = 1, \dots, J.$$

For the numerical implementation of the inverse problem, we need to discretize the equations (2.7) and (2.8). In this paper, we use the method proposed in [52] for discretization. We divide the entire space  $\mathbb{R}^n$  into open boxes with a given small number  $h > 0$ :

$$B_{p,h} := \{x = (x_1, \dots, x_n) \in \mathbb{R}^n : (p_k - \frac{1}{2})h < x_k < (p_k + \frac{1}{2})h, k = 1, \dots, n\},$$

where  $p = (p_1, \dots, p_n) \in \mathbb{Z}^n$  and  $ph$  represents the center point of  $B_{p,h}$ . Since the support of  $m(x)$  is assumed to be compact, we can choose a sufficiently large  $N \in \mathbb{N}$  and an open bounded set  $G \subset \mathbb{R}^n$  (independent of  $h$ ) such that

$$\text{supp}(m) \subset \bigcup_{p \in \mathbb{Z}_N^n} \overline{B}_{p,h} \subset G,$$

where

$$\mathbb{Z}_N^n := \{p = (p_1, \dots, p_n) \in \mathbb{Z}^n : -\frac{N}{2} < p_k \leq \frac{N}{2}, k = 1, \dots, n\}.$$

Further, define

$$\Phi_{p,h} := \begin{cases} \Phi(\kappa|p|h), & 0 \neq p \in \mathbb{Z}_N^n, \\ 0, & p = 0. \end{cases}$$

Then the state equation (2.8) is discretized as the discrete system

$$(2.9) \quad \omega_{j,p,h} = m_{p,h}u_j^i(ph) + h^n m_{p,h} \kappa^n \sum_{k \in \mathbb{Z}_N^n} \Phi_{p-k,h} \omega_{j,k,h}, \quad p \in \mathbb{Z}_N^n, \quad j = 1, \dots, J,$$

where  $m_{p,h}$  is the value of the contrast  $m(x)$  at  $ph$  as in [52]. We sort the points of  $\mathbb{Z}_N^n$  by  $p^1, \dots, p^M$ , with  $M = N^n$ , in a fixed order, e.g., the lexicographic order, and rewrite the equation (2.9) as the discrete state equation

$$(2.10) \quad \boldsymbol{\omega}_j = \mathbf{m} \odot \mathbf{u}_j^i + \mathbf{m} \odot T \boldsymbol{\omega}_j, \quad j = 1, \dots, J,$$

where

$$\begin{aligned}\mathbf{m} &:= (m_{p^1,h}, \dots, m_{p^M,h})^\top \in \mathbb{C}^M, \\ \mathbf{u}_j^i &:= (u_j^i(p^1h), \dots, u_j^i(p^Mh))^\top \in \mathbb{C}^M, \\ \boldsymbol{\omega}_j &:= (\omega_{j,p^1,h}, \dots, \omega_{j,p^M,h})^\top \in \mathbb{C}^M,\end{aligned}$$

$$T := \kappa^n h^n \begin{pmatrix} \Phi_{p^1-p^1,h} & \cdots & \Phi_{p^1-p^M,h} \\ \vdots & \ddots & \vdots \\ \Phi_{p^M-p^1,h} & \cdots & \Phi_{p^M-p^M,h} \end{pmatrix} \in \mathbb{C}^{M \times M},$$

and the operation  $\odot$  denotes the element-wise multiplication. Define  $D(\mathbf{m}) := \text{diag}(\mathbf{m})$  as a diagonal matrix and denote by  $I_M$  the identity matrix of order  $M$ . Then (2.10) can be rewritten in the matrix form:

$$(2.11) \quad [I_M - D(\mathbf{m})T]\boldsymbol{\omega}_j = D(\mathbf{m})\mathbf{u}_j^i, \quad j = 1, \dots, J.$$

*Remark 2.1.* Through the paper, we assume that  $m(x)$  is a piecewise smooth function with a compact support and satisfies the condition mentioned in [52, Theorem 2.1]. Further, assume that the homogeneous integral equation corresponding to (2.6) possesses only the trivial solution. Then, it has been shown in [52, Theorem 2.1] that for each  $j = 1, \dots, J$  and for any sufficiently small  $h > 0$ , the discrete system [52, Equation (8)]:

$$(2.12) \quad u_{j,p,h} = u_j^i(ph) + h^n \sum_{k \in \mathbb{Z}_N^n} \Phi_{p-k,h} m_{k,h} u_{j,k,h}, \quad p \in \mathbb{Z}_N^n,$$

or

$$[I_M - TD(\mathbf{m})]\mathbf{u}_j = \mathbf{u}_j^i \quad \text{with } \mathbf{u}_j := (u_{j,p^1,h}, \dots, u_{j,p^M,h})^\top \in \mathbb{C}^M$$

is uniquely solvable, and the error between  $u_j(ph)$  (the solution of (2.6)) and  $u_{j,p,h}$  (the solution of (2.12)) is  $O(h^2(1 + |\ln h|))$ . Thus, the matrix  $[I_M - D(\mathbf{m})T] = [I_M - TD(\mathbf{m})]^\top$  in (2.11) is invertible, and the error between  $\omega_j(ph)$  (the solution of (2.8)) and  $\omega_{j,p,h}$  (the solution of (2.9)) is also  $O(h^2(1 + |\ln h|))$ .

We now discretize the data equation (2.7). Given  $Q \in \mathbb{N}^+$ , we choose different observation directions  $\hat{x}^1, \dots, \hat{x}^Q$ . Then, for each  $j = 1, \dots, J$ , the data equation (2.7) can be rewritten as

$$(2.13) \quad \mathbf{u}_j^\infty = T^\infty \boldsymbol{\omega}_j + \boldsymbol{\varepsilon}_{j,h} \approx T^\infty \boldsymbol{\omega}_j \quad \text{for sufficiently small } h > 0,$$

since the infinity norm of  $\boldsymbol{\varepsilon}_{j,h}$  tends to 0 as  $h \rightarrow +0$  (see [51, 52]). Here,

$$\mathbf{u}_j^\infty := (u_j^\infty(\hat{x}^1), \dots, u_j^\infty(\hat{x}^Q))^\top \in \mathbb{C}^Q$$

and

$$T^\infty := \theta_{n,\kappa} h^n \begin{pmatrix} e^{-i\kappa\hat{x}^1 \cdot p^1 h} & \cdots & e^{-i\kappa\hat{x}^1 \cdot p^M h} \\ \vdots & \ddots & \vdots \\ e^{-i\kappa\hat{x}^Q \cdot p^1 h} & \cdots & e^{-i\kappa\hat{x}^Q \cdot p^M h} \end{pmatrix} \in \mathbb{C}^{Q \times M}.$$

Therefore, we assume that  $h > 0$  is sufficiently small throughout the paper.

Let  $\mathbf{u}_j^{\infty,\delta}$  denote the noisy data satisfying that

$$(2.14) \quad \|\mathbf{u}_j^{\infty,\delta} - \mathbf{u}_j^\infty\| \leq \delta, \quad j = 1, \dots, J.$$

Hereafter,  $\|\cdot\|$  represents the  $\ell_2$ -norm of a vector  $\|\cdot\|_2$  unless otherwise specified. Then the (discrete) *inverse medium scattering problem* considered in this paper is as follows: Given  $\mathbf{u}_j^i$  and for a fixed and sufficiently small  $h$ , reconstruct  $\mathbf{m}$  from the data  $\mathbf{u}_j^{\infty,\delta}$ ,  $j = 1, \dots, J$ .

**3. The original CSI and SOM methods for inverse medium scattering problems.** In this section, we present the original CSI method [53] and the original SOM [15] for solving the inverse medium scattering problem.

The original CSI method [53] updates  $\omega_j$  and  $\mathbf{m}$  alternatively to minimize the following objective function, which is a weighted sum of the errors between the state equation (2.10) and the data equation (2.13) with  $j = 1, \dots, J$ :

$$(3.1) \quad F^{csi}(\omega_1, \dots, \omega_J, \mathbf{m})$$

$$= \sum_{j=1}^J \eta_{s,j} \|\mathbf{m} \odot \mathbf{u}_j^i + \mathbf{m} \odot T\omega_j - \omega_j\|^2 + \sum_{j=1}^J \eta_{d,j} \|\mathbf{u}_j^{\infty,\delta} - T^\infty \omega_j\|^2,$$

where  $\eta_{s,j}$  and  $\eta_{d,j}$  are positive weights. In [53], the weights are chosen as

$$\eta_{s,1} = \dots = \eta_{s,J} = \left( \sum_{j=1}^J \|\mathbf{m} \odot \mathbf{u}_j^i\|^2 \right)^{-1}, \quad \eta_{d,1} = \dots = \eta_{d,J} = \left( \sum_{j=1}^J \|\mathbf{u}_j^{\infty,\delta}\|^2 \right)^{-1}.$$

Note that the weights  $\eta_{s,j}$  are functions of  $\mathbf{m}$ . When  $\omega_j = 0$ , the first and second terms on the right-hand side of (3.1) are both 1, so the weights  $\eta_{s,j}$  and  $\eta_{d,j}$  balance the errors between these two terms.

The CSI method consists of constructing the sequences  $\{\omega_j^{(r)}\}_{r \in \mathbb{N}}$  and  $\{\mathbf{m}^{(r)}\}_{r \in \mathbb{N}}$  for updating  $\omega_j$  and  $\mathbf{m}$ , respectively, as follows.

- Updating  $\omega_j^{(r+1)}$ : Calculate the gradient  $g_j^{(r)} = \nabla_{\omega_j} F^{csi}$  evaluated at  $\omega_j^{(r)}$  and  $\mathbf{m}^{(r)}$  (see Definition 5.1). Determine the Polak–Ribiére conjugate gradient search directions  $v_j^{(r)} = g_j^{(r)} + \text{Re} [\langle g_j^{(r)}, g_j^{(r)} - g_j^{(r-1)} \rangle] \|g_j^{(r)}\|^{-2} v_j^{(r-1)}$ . Let  $\omega_j^{(r+1)} = \omega_j^{(r)} + s_j^{(r)} v_j^{(r)}$  with the step size  $s_j^{(r)}$  to be determined. Then the objective function becomes quadratic in terms of  $s_j^{(r)}$ , which can be easily solved for  $s_j^{(r)}$  as in [53, 54].
- Updating  $\mathbf{m}^{(r+1)}$ : Regarding  $\eta_{s,j}$  as a constant  $\left( \sum_{j=1}^J \|\mathbf{m}^{(r)} \odot \mathbf{u}_j^i\|^2 \right)^{-1}$ , finding the optimal  $\mathbf{m}^{(r+1)}$  is equivalent to minimizing the following function with respect to  $\mathbf{m}$ :

$$\sum_{j=1}^J \eta_{s,j} \|\mathbf{m} \odot \mathbf{u}_j^i + \mathbf{m} \odot T\omega_j^{(r+1)} - \omega_j^{(r+1)}\|^2.$$

Denote by  $(\xi)_\ell$  the  $\ell$ -th element of the vector  $\xi$ . Then the solution  $\mathbf{m}^{(r+1)}$  can be given explicitly with its  $\ell$ -th element

$$(3.2) \quad (\mathbf{m}^{(r+1)})_\ell = \left[ \sum_{j=1}^J \overline{(\mathbf{u}_j^{(r+1)})_\ell} (\omega_j^{(r+1)})_\ell \right] \Big/ \left[ \sum_{j=1}^J |(\mathbf{u}_j^{(r+1)})_\ell|^2 \right],$$

where  $\mathbf{u}_j^{(r+1)} = \mathbf{u}_j^i + T\omega_j^{(r+1)}$ .

From the updating process of the CSI algorithm, it is seen that the weights  $\eta_{s,j}$  are regarded as the constant  $\left(\sum_{j=1}^J \|\mathbf{m}^{(r)} \odot \mathbf{u}_j^i\|^2\right)^{-1}$  in updating  $\omega_j^{(r+1)}$  and  $\mathbf{m}^{(r+1)}$  at the  $r$ -th iteration. This means that the objective function of the CSI method is always changing (since the values of  $\eta_{s,j}$  are different at each iteration), making the convergence analysis of the CSI method more complicated. Thus, in this paper, we only consider the convergence of the CSI method in the case when the weights  $\eta_{s,j}$  and  $\eta_{d,j}$  are positive constants. It should be mentioned that the CSI method with positive constant weights actually works well in practical computation, as demonstrated in our numerical experiments. For example, if the contrast  $\mathbf{m}$  has a good initial guess  $\mathbf{m}^{(0)}$ , then we can set  $\eta_{s,j} = \left(\sum_{j=1}^J \|\mathbf{m}^{(0)} \odot \mathbf{u}_j^i\|^2\right)^{-1}$ . Thus the weights remain unchanged during the updating process. Our numerical experiments show that the weights so chosen have very little impact on the reconstruction results.

Write  $F^{csi}(\omega_1, \dots, \omega_J, \mathbf{m}) = \sum_{j=1}^J F_j^{csi}(\omega_j, \mathbf{m})$  with

$$F_j^{csi}(\omega_j, \mathbf{m}) := \eta_{s,j} \|\mathbf{m} \odot \mathbf{u}_j^i + \mathbf{m} \odot T\omega_j - \omega_j\|^2 + \eta_{d,j} \|\mathbf{u}_j^{\infty, \delta} - T^\infty \omega_j\|^2.$$

Then the updating process of the CSI method can be written as

$$(3.3) \quad \omega_j^{(r+1)} = \omega_j^{(r)} + s_j^{(r)} \mathbf{v}_j^{(r)}, \quad j = 1, \dots, J,$$

$$(3.4) \quad \mathbf{m}^{(r+1)} \in \arg \min_{\mathbf{m}} F^{csi}(\omega_1^{(r+1)}, \dots, \omega_J^{(r+1)}, \mathbf{m}).$$

Here, the updating direction  $\mathbf{v}_j^{(r)}$  is the Polak–Ribi  re conjugate gradient direction and  $s_j^{(r)}$  is the optimal step size given by the solution of the problem

$$(3.5) \quad s_j^{(r)} \in \arg \min_s F_j^{csi}(\omega_j^{(r)} + s \mathbf{v}_j^{(r)}, \mathbf{m}^{(r)}).$$

The explicit solution of (3.4) is given in (3.2), whilst (3.5) can be solved explicitly as in [53, 54, 55].

We now present the SOM method [15]. Recall the data equation (2.13) and consider the Singular Value Decomposition (SVD) of  $T^\infty = \sum_k \mathbf{u}_k \lambda_k \mathbf{v}_k^*$  with the singular values  $\lambda_1 \geq \dots \geq \lambda_{L_0} > \lambda_{L_0+1} = \dots = \lambda_M = 0$  being placed in a non-increasing order. Then we split  $\omega_j$  up into two parts:

$$\omega_j = \omega_j^s + \omega_j^n,$$

where  $\omega_j^s$  (the signal of  $\omega_j$ ) is spanned by the first  $L_\alpha$  right singular vectors  $\mathbf{v}_k$  ( $k \leq L_\alpha$ ), and  $\omega_j^n$  (the noise of  $\omega_j$ ) is spanned by the remaining  $M - L_\alpha$  right singular vectors  $\mathbf{v}_k$  ( $k > L_\alpha$ ). Here,  $L_\alpha$  is a predefined integer selected in  $[1, L_0]$  and  $\omega_j^s$  is uniquely determined as follows:

$$(3.6) \quad \omega_j^s = \sum_{k=1}^{L_\alpha} \frac{\langle \mathbf{u}_j^{\infty, \delta}, \mathbf{u}_k \rangle}{\lambda_k} \mathbf{v}_k.$$

Thus only  $\omega_j^n = \alpha_1 \mathbf{v}_{L_\alpha+1} + \dots + \alpha_{M-L_\alpha} \mathbf{v}_M$  needs to be solved, that is,

$$\omega_j^n = (\mathbf{v}_{L_\alpha+1}, \dots, \mathbf{v}_M) \boldsymbol{\alpha}_j$$

with an  $(M - L_\alpha)$ -dimensional vector  $\boldsymbol{\alpha}_j$  to be determined. Let  $V^n \in \mathbb{C}^{M \times (M - L_\alpha)}$  denote the matrix  $(\mathbf{v}_{L_\alpha+1}, \dots, \mathbf{v}_M)$ . Then

$$(3.7) \quad \boldsymbol{\omega}_j = \boldsymbol{\omega}_j^s + V^n \boldsymbol{\alpha}_j, \quad j = 1, \dots, J,$$

and the objective functional of SOM is

$$(3.8) \quad \begin{aligned} F^{som}(\boldsymbol{\alpha}_1, \dots, \boldsymbol{\alpha}_J, \mathbf{m}) &= \sum_{j=1}^J \eta_{s,j} \|\mathbf{m} \odot \mathbf{u}_j^i + \mathbf{m} \odot T(\boldsymbol{\omega}_j^s + V^n \boldsymbol{\alpha}_j) - (\boldsymbol{\omega}_j^s + V^n \boldsymbol{\alpha}_j)\|^2 \\ &\quad + \sum_{j=1}^J \eta_{d,j} \|\mathbf{u}_j^{\infty, \delta} - T^\infty \boldsymbol{\omega}_j^s - T^\infty V^n \boldsymbol{\alpha}_j\|^2, \end{aligned}$$

where  $\eta_{s,j}$  and  $\eta_{d,j}$  are positive weights. In [15],  $\eta_{s,j}$  and  $\eta_{d,j}$  are taken to be some real constants.

The SOM method constructs the sequences  $\{\boldsymbol{\alpha}_j^{(r)}\}_{r \in \mathbb{N}}$  and  $\{\mathbf{m}^{(r)}\}_{r \in \mathbb{N}}$  for updating  $\boldsymbol{\alpha}_j$  and  $\mathbf{m}$ , respectively, as follows.

- Updating  $\boldsymbol{\alpha}_j^{(r+1)}$ : Calculate the gradient  $g_j^{(r)} = \nabla_{\boldsymbol{\alpha}_j} F^{som}$  evaluated at  $\boldsymbol{\alpha}_j^{(r)}$  and  $\mathbf{m}^{(r)}$  (see Definition 5.1). Determine the Polak–Ribi  re conjugate gradient search directions  $\rho_j^{(r)} = g_j^{(r)} + \text{Re} [\langle g_j^{(r)}, g_j^{(r)} - g_j^{(r-1)} \rangle] \|g_j^{(r)}\|^{-2} \rho_j^{(r-1)}$ . Set  $\boldsymbol{\alpha}_j^{(r+1)} = \boldsymbol{\alpha}_j^{(r)} + s_j^{(r)} \rho_j^{(r)}$  with the step size  $s_j^{(r)}$  to be determined. Then the objective function becomes quadratic in terms of  $s_j^{(r)}$ , which can be easily solved for  $s_j^{(r)}$  as in [14, 15].
- Updating  $\mathbf{m}^{(r+1)}$ : The weights  $\eta_{s,j}$  are constants in the SOM method, so the optimal  $\mathbf{m}^{(r+1)}$  is the solution to the optimization problem

$$\mathbf{m}^{(r+1)} \in \arg \min_{\mathbf{m}} F^{som}(\boldsymbol{\alpha}_1^{(r)}, \dots, \boldsymbol{\alpha}_J^{(r)}, \mathbf{m}).$$

The solution  $\mathbf{m}^{(r+1)}$  can be explicitly given with its  $\ell$ -th element

$$(3.9) \quad (\mathbf{m}^{(r+1)})_\ell = \left[ \sum_{j=1}^J \overline{(\mathbf{u}_j^{(r+1)})_\ell} (\boldsymbol{\omega}_j^{(r+1)})_\ell \right] \Big/ \left[ \sum_{j=1}^J |(\mathbf{u}_j^{(r+1)})_\ell|^2 \right],$$

where  $\boldsymbol{\omega}_j^{(r+1)} = \boldsymbol{\omega}_j^s + V^n \boldsymbol{\alpha}_j^{(r+1)}$  and  $\mathbf{u}_j^{(r+1)} = \mathbf{u}_j^i + T \boldsymbol{\omega}_j^{(r+1)}$ .

Similarly, we write  $F^{som}(\boldsymbol{\alpha}_1, \dots, \boldsymbol{\alpha}_J, \mathbf{m}) = \sum_{j=1}^J F_j^{som}(\boldsymbol{\alpha}_j, \mathbf{m})$  with

$$\begin{aligned} F_j^{som}(\boldsymbol{\alpha}_j, \mathbf{m}) &:= \eta_{s,j} \|\mathbf{m} \odot \mathbf{u}_j^i + \mathbf{m} \odot T(\boldsymbol{\omega}_j^s + V^n \boldsymbol{\alpha}_j) - (\boldsymbol{\omega}_j^s + V^n \boldsymbol{\alpha}_j)\|^2 \\ &\quad + \eta_{d,j} \|\mathbf{u}_j^{\infty, \delta} - T^\infty \boldsymbol{\omega}_j^s - T^\infty V^n \boldsymbol{\alpha}_j\|^2. \end{aligned}$$

Then the updating process of the SOM method can be written as

$$(3.10) \quad \boldsymbol{\alpha}_j^{(r+1)} = \boldsymbol{\alpha}_j^{(r)} + s_j^{(r)} \rho_j^{(r)}, \quad j = 1, \dots, J,$$

$$(3.11) \quad \mathbf{m}^{(r+1)} \in \arg \min_{\mathbf{m}} F^{som}(\boldsymbol{\alpha}_1^{(r+1)}, \dots, \boldsymbol{\alpha}_J^{(r+1)}, \mathbf{m}).$$

Here, the updating direction  $\rho_j^{(r)}$  is the Polak–Ribi  re Conjugate Gradient (PR-CG) direction and  $s_j^{(r)}$  is the optimal step size given by the solution of the problem

$$(3.12) \quad s_j^{(r)} \in \arg \min_s F_j^{som}(\boldsymbol{\alpha}_j^{(r)} + s \rho_j^{(r)}, \mathbf{m}^{(r)}).$$

The explicit solution of (3.11) is given in (3.9), whilst (3.12) can be given explicitly as in [15].

It should be noted that the convergence of the original CSI and SOM methods remains an open problem. In fact, by the numerical experiments in Section 6 it seems that the original CSI and SOM methods may not converge in the case with noisy measurement data. In the next section, we propose iteratively regularized CSI and SOM algorithms with a novel  $\ell_1$  proximal term as the iteratively regularized term, which have a similar computational complexity to the original CSI and SOM algorithms, respectively, and will be proved to be globally convergent under natural and weak conditions on the original objective function.

**4. Iteratively regularized CSI and SOM algorithms.** In the rest of this paper, we assume that the weights  $\eta_{s,j}$  and  $\eta_{d,j}$  in the objective functions  $F^{csi}$  and  $F^{som}$  (see (3.1) and (3.8)) are positive constants.

Recall that  $F^{csi}$  is a function mapping  $\mathbb{C}^{MJ} \times \mathbb{C}^M$  to  $\mathbb{R}$ . As for the updating equations (3.3) and (3.4) in the CSI method,  $\omega_j^{(r+1)}$  given by (3.3) and (3.5) can be regarded as an approximate solution of the problem

$$(4.1) \quad \omega_j^{(r+1)} \in \arg \min_{\omega_j} F_j^{csi}(\omega_j, \mathbf{m}^{(r)}), \quad j = 1, \dots, J.$$

The only difference is that  $\omega_j^{(r+1)}$  given by (3.3) and (3.5) solves (4.1) along one conjugate gradient direction  $\mathbf{v}_j^{(r)}$  instead of on the whole space  $\mathbb{C}^M$ . By letting  $\omega \in \mathbb{C}^{MJ}$  represent the variables  $(\omega_1, \dots, \omega_J)$ , (4.1) is equivalent to

$$(4.2) \quad \omega^{(r+1)} \in \arg \min_{(\omega_1, \dots, \omega_J)} \sum_{j=1}^J F_j^{csi}(\omega_j, \mathbf{m}^{(r)}) = \arg \min_{\omega} F^{csi}(\omega, \mathbf{m}^{(r)}).$$

The subproblem (3.4) can be rewritten as

$$(4.3) \quad \mathbf{m}^{(r+1)} \in \arg \min_{\mathbf{m}} F^{csi}(\omega^{(r+1)}, \mathbf{m}).$$

We now consider the following iteratively regularized CSI method:

$$(4.4) \quad \omega^{(r+1)} \in \arg \min_{\omega} F^{csi}(\omega, \mathbf{m}^{(r)}) + \gamma \|\omega - \omega^{(r)}\|_1,$$

$$(4.5) \quad \mathbf{m}^{(r+1)} \in \arg \min_{\mathbf{m}} F^{csi}(\omega^{(r+1)}, \mathbf{m}) + \beta \|\mathbf{m} - \mathbf{m}^{(r)}\|_1.$$

Here and throughout the paper,  $\|\cdot\|_1$  represents the  $\ell_1$ -norm of a vector. The subproblem (4.4) can be solved approximately by the one-step PR-CG method:

$$(4.6) \quad \omega_j^{(r+1)} = \omega_j^{(r)} + s_j^{(r)} \mathbf{v}_j^{(r)}, \quad j = 1, \dots, J,$$

$$(4.7) \quad s_j^{(r)} \in \arg \min_s F_j^{csi}(\omega_j^{(r)} + s \mathbf{v}_j^{(r)}, \mathbf{m}^{(r)}) + \gamma \|s \mathbf{v}_j^{(r)}\|_1.$$

Here, the update direction  $\mathbf{v}_j^{(r)}$  is the PR-CG direction:

$$(4.8) \quad \mathbf{v}_j^{(r)} = \begin{cases} g_j^{(0)}, & r = 0, \\ g_j^{(r)} + \frac{\operatorname{Re} \langle g_j^{(r)}, g_j^{(r)} - g_j^{(r-1)} \rangle}{\|g_j^{(r-1)}\|^2} \mathbf{v}_j^{(r-1)}, & r \geq 1 \text{ and } g_j^{(r-1)} \neq 0, \\ g_j^{(r)}, & r \geq 1 \text{ and } g_j^{(r-1)} = 0, \end{cases}$$

with  $g_j^{(r)} = \nabla_{\omega_j} F_j^{csi}(\omega_j^{(r)}, \mathbf{m}^{(r)})$  given as in Section 3. The step size  $s_j^{(r)}$ , that is, the solution of the problem (4.7) has a closed-form expression which can be obtained as follows.

Define the state error by

$$E_{s,j}^{(r)} := \mathbf{m}^{(r)} \odot \mathbf{u}_j^i + \mathbf{m}^{(r)} \odot T\omega_j^{(r)} - \omega_j^{(r)}$$

and the data error by

$$E_{d,j}^{(r)} := \mathbf{u}_j^{\infty, \delta} - T^\infty \omega_j^{(r)}.$$

Then the step size constant  $s_j^{(r)}$  is the solution of the optimization problem

$$\begin{aligned} s_j^{(r)} \in \arg \min_s & \left\{ \eta_{s,j} \|E_{s,j}^{(r)} + s(\mathbf{m}^{(r)} \odot T\mathbf{v}_j^{(r)} - \mathbf{v}_j^{(r)})\|^2 \right. \\ & \left. + \eta_{d,j} \|E_{d,j}^{(r)} - sT^\infty \mathbf{v}_j^{(r)}\|^2 + \gamma \|\mathbf{v}_j^{(r)}\|_1 |s| \right\}, \end{aligned}$$

which is given explicitly by

$$(4.9) \quad s_j^{(r)} = \begin{cases} 0, & \|\mathbf{m}^{(r)} \odot T\mathbf{v}_j^{(r)} - \mathbf{v}_j^{(r)}\| = \|T^\infty \mathbf{v}_j^{(r)}\| = 0, \\ S_\tau(z), & \text{otherwise.} \end{cases}$$

Here,  $\tau$  and  $z$  are given by

$$\begin{aligned} \tau &= \frac{\gamma \|\mathbf{v}_j^{(r)}\|_1}{2\eta_{s,j} \|\mathbf{v}_j^{(r)} - \mathbf{m}^{(r)} \odot T\mathbf{v}_j^{(r)}\|^2 + 2\eta_{d,j} \|T^\infty \mathbf{v}_j^{(r)}\|^2}, \\ z &= \frac{\eta_{s,j} \langle E_{s,j}^{(r)}, \mathbf{v}_j^{(r)} - \mathbf{m}^{(r)} \odot T\mathbf{v}_j^{(r)} \rangle + \eta_{d,j} \langle E_{d,j}^{(r)}, T^\infty \mathbf{v}_j^{(r)} \rangle}{\eta_{s,j} \|\mathbf{v}_j^{(r)} - \mathbf{m}^{(r)} \odot T\mathbf{v}_j^{(r)}\|^2 + \eta_{d,j} \|T^\infty \mathbf{v}_j^{(r)}\|^2} \\ &= \frac{-\langle g_j^{(r)}, \mathbf{v}_j^{(r)} \rangle}{2\eta_{s,j} \|\mathbf{v}_j^{(r)} - \mathbf{m}^{(r)} \odot T\mathbf{v}_j^{(r)}\|^2 + 2\eta_{d,j} \|T^\infty \mathbf{v}_j^{(r)}\|^2} \end{aligned}$$

and  $S_\tau(\cdot)$  is a complex soft-threshold function defined by

$$S_\tau(a) := \begin{cases} (|a| - \tau)a/|a|, & |a| > \tau, \\ 0, & \text{otherwise.} \end{cases}$$

The subproblem (4.5) is a special LASSO problem which can be solved exactly as follows.

Let  $\mathbf{u}_j^{(r+1)} = \mathbf{u}_j^i + T\omega_j^{(r+1)}$ . Then, by the definition (3.1) of  $F^{csi}(\omega, \mathbf{m})$  the problem (4.3) is equivalent to the following problem

$$\mathbf{m}^{(r+1)} \in \arg \min_{\mathbf{m}} \sum_{j=1}^J \eta_{s,j} \|\mathbf{m} \odot \mathbf{u}_j^{(r+1)} - \omega_j^{(r+1)}\|^2 + \beta \|\mathbf{m} - \mathbf{m}^{(r)}\|_1.$$

The  $\ell$ -th element of the solution  $\mathbf{m}^{(r+1)}$  can be obtained as

$$(4.10) \quad (\mathbf{m}^{(r+1)})_\ell = \begin{cases} (\mathbf{m}^{(r)})_\ell, & (\mathbf{u}_j^{(r+1)})_\ell = 0 \text{ for all } j = 1, \dots, J, \\ (\mathbf{m}^{(r)})_\ell + S_\tau(z - (\mathbf{m}^{(r)})_\ell), & \text{otherwise,} \end{cases}$$

with

$$\tau = \frac{\beta}{2 \sum_{j=1}^J \eta_{s,j} |(\mathbf{u}_j^{(r+1)})_\ell|^2}, \quad z = \frac{\sum_{j=1}^J \eta_{s,j} \overline{(\mathbf{u}_j^{(r+1)})_\ell} (\boldsymbol{\omega}_j^{(r+1)})_\ell}{\sum_{j=1}^J \eta_{s,j} |(\mathbf{u}_j^{(r+1)})_\ell|^2}.$$

To sum up, the proposed iteratively regularized CSI (IRCSI) algorithm consists of (4.6), (4.8), (4.9) and (4.10) and is presented in Algorithm 4.1.

It should be remarked that an  $\ell_1$  proximal term was also used in [23] for regularized variational image restoration models with smoothly truncated regularizer functions. It should be remarked further that regularized CSI methods have also been proposed in [54] with the regularizing term being the standard TV term and in [61] with the regularization term being the Bregman distance induced by a general uniformly convex functional.

Similarly, we consider the iteratively regularized SOM method:

$$(4.11) \quad \boldsymbol{\alpha}^{(r+1)} \in \arg \min_{\boldsymbol{\alpha}} F^{som}(\boldsymbol{\alpha}, \mathbf{m}^{(r)}) + \gamma \|\boldsymbol{\alpha} - \boldsymbol{\alpha}^{(r)}\|_1,$$

$$(4.12) \quad \mathbf{m}^{(r+1)} \in \arg \min_{\mathbf{m}} F^{som}(\boldsymbol{\alpha}^{(r+1)}, \mathbf{m}) + \beta \|\mathbf{m} - \mathbf{m}^{(r)}\|_1.$$

We still use the one-step PR-CG method to solve the subproblem (4.11) approximately, that is,

$$(4.13) \quad \boldsymbol{\alpha}_j^{(r+1)} = \boldsymbol{\alpha}_j^{(r)} + s_j^{(r)} \boldsymbol{\rho}_j^{(r)}, \quad j = 1, \dots, J,$$

$$(4.14) \quad s_j^{(r)} \in \arg \min_s F_j^{som}(\boldsymbol{\alpha}_j^{(r)} + s \boldsymbol{\rho}_j^{(r)}, \mathbf{m}^{(r)}) + \gamma \|s \boldsymbol{\rho}_j^{(r)}\|_1.$$

Here,

$$(4.15) \quad \boldsymbol{\rho}_j^{(r)} = \begin{cases} \mathbf{g}_j^{(0)}, & r = 0, \\ \mathbf{g}_j^{(r)} + \frac{\operatorname{Re} \langle \mathbf{g}_j^{(r)}, \mathbf{g}_j^{(r)} - \mathbf{g}_j^{(r-1)} \rangle}{\|\mathbf{g}_j^{(r-1)}\|^2} \boldsymbol{\rho}_j^{(r-1)}, & r \geq 1 \text{ and } \mathbf{g}_j^{(r-1)} \neq 0, \\ \mathbf{g}_j^{(r)}, & r \geq 1 \text{ and } \mathbf{g}_j^{(r-1)} = 0, \end{cases}$$

with  $\mathbf{g}_j^{(r)} = \nabla_{\boldsymbol{\alpha}_j} F_j^{som}(\boldsymbol{\alpha}_j^{(r)}, \mathbf{m}^{(r)})$  given as in Section 3. Let  $\boldsymbol{\omega}_j^{(r)} = \boldsymbol{\omega}_j^s + V^n \boldsymbol{\alpha}_j^{(r)}$ ,  $\mathbf{u}_j^{(r+1)} = \mathbf{u}_j^i + T \boldsymbol{\omega}_j^{(r+1)}$ . Then the step size  $s_j^{(r)}$ , that is, the solution of the problem (4.14) is given by

$$(4.16) \quad s_j^{(r)} = \begin{cases} 0, & \|V^n \boldsymbol{\rho}_j^{(r)} - \mathbf{m}^{(r)} \odot TV^n \boldsymbol{\rho}_j^{(r)}\| = \|TV^n \boldsymbol{\rho}_j^{(r)}\| = 0, \\ S_\tau(z), & \text{otherwise,} \end{cases}$$

where

$$\begin{aligned} \tau &= \frac{\gamma \|\boldsymbol{\rho}_j^{(r)}\|_1}{2\eta_{s,j} \|V^n \boldsymbol{\rho}_j^{(r)} - \mathbf{m}^{(r)} \odot TV^n \boldsymbol{\rho}_j^{(r)}\|^2 + 2\eta_{d,j} \|TV^n \boldsymbol{\rho}_j^{(r)}\|^2}, \\ z &= \frac{-\langle \mathbf{g}_j^{(r)}, \boldsymbol{\rho}_j^{(r)} \rangle}{2\eta_{s,j} \|V^n \boldsymbol{\rho}_j^{(r)} - \mathbf{m}^{(r)} \odot TV^n \boldsymbol{\rho}_j^{(r)}\|^2 + 2\eta_{d,j} \|TV^n \boldsymbol{\rho}_j^{(r)}\|^2}. \end{aligned}$$

The problem (4.12) has also an explicit solution with its  $\ell$ -th element given by

(4.17)

$$(\mathbf{m}^{(r+1)})_\ell = \begin{cases} (\mathbf{m}^{(r)})_\ell, & (\mathbf{u}_j^{(r+1)})_\ell = 0 \text{ for all } j = 1, \dots, J, \\ (\mathbf{m}^{(r)})_\ell + S_\tau(z - (\mathbf{m}^{(r)})_\ell), & \text{otherwise,} \end{cases}$$

with

$$\tau = \frac{\beta}{2 \sum_{j=1}^J \eta_{s,j} |(\mathbf{u}_j^{(r+1)})_\ell|^2}, \quad z = \frac{\sum_{j=1}^J \eta_{s,j} \overline{(\mathbf{u}_j^{(r+1)})_\ell} (\omega_j^{(r+1)})_\ell}{\sum_{j=1}^J \eta_{s,j} |(\mathbf{u}_j^{(r+1)})_\ell|^2}.$$

To sum up, the proposed iteratively regularized SOM (IRSOM) algorithm consists of (4.13), (4.15), (4.16) and (4.17) and is presented in Algorithm 4.2.

Note that, in the case when  $\gamma = \beta = 0$ , our IRCSI and IRSOM algorithms are reduced to the original CSI and SOM algorithms, respectively. Further, similarly to the original CSI and SOM algorithms, the IRCSI and IRSOM algorithms also have closed-form solutions and thus have a similar computational complexity to the original CSI algorithm [53] and SOM algorithm [15], respectively. In the next section, we will give a rigorous convergence analysis of the IRCSI and IRSOM algorithms.

---

**Algorithm 4.1** The IRCSI algorithm

---

**Input:** wave number  $k$ , linear operators  $T$  and  $T^\infty$ ,  
 positive constants  $\gamma, \beta, \eta_{s,j}, \eta_{d,j}$ ,  $j = 1, \dots, J$ ,  
 incident wave  $\mathbf{u}_j^i$ , measurement data  $\mathbf{u}_j^{\infty,\delta}$ ,  $j = 1, \dots, J$ .

- 1: **Initialize:**  $r = 0$  and  $(\omega_1^{(0)}, \dots, \omega_J^{(0)}, \mathbf{m}^{(0)})$  is given by back-propagation [53, 54, 55].
- 2: **while** (the termination criterion is not satisfied) **do**
- 3: For all  $j = 1, \dots, J$ , compute the gradient  $g_j^{(r)} = \nabla_{\omega_j} F^{csi}(\omega^{(r)}, \mathbf{m}^{(r)})$  and then determine the PR-CG search direction by (4.8).
- 4: Update  $\omega_j^{(r+1)}$  as  $\omega_j^{(r+1)} = \omega_j^{(r)} + s_j^{(r)} \mathbf{v}_j^{(r)}$  with  $s_j^{(r)}$  given by (4.9).
- 5: Update  $\mathbf{m}^{(r+1)}$  by (4.10).
- 6:  $r = r + 1$ .
- 7: **end while**

---

**Algorithm 4.2** The IRSOM algorithm

---

**Input:** wave number  $k$ , linear operators  $T$  and  $T^\infty$ ,  
 positive constants  $\gamma, \beta, \eta_{s,j}, \eta_{d,j}$ ,  $j = 1, \dots, J$ ,  
 incident wave  $\mathbf{u}_j^i$ , measurement data  $\mathbf{u}_j^{\infty,\delta}$ ,  $j = 1, \dots, J$ ,  
 the vector  $\omega_j^s$  and the matrix  $V^n \in \mathbb{C}^{M \times (M-L_\alpha)}$  given as in (3.7).

- 1: **Initialize:**  $r = 0$ ,  $\alpha_j^{(0)} = 0$ , and  $\mathbf{m}^{(0)}$  is given by back-propagation [53, 54, 55].
- 2: **while** (the termination criterion is not satisfied) **do**
- 3: For all  $j = 1, \dots, J$ , compute the gradient  $g_j^{(r)} = \nabla_{\alpha_j} F^{som}(\alpha^{(r)}, \mathbf{m}^{(r)})$  and then determine the PR-CG search direction by (4.15).
- 4: Update  $\alpha_j^{(r+1)}$  by  $\alpha_j^{(r+1)} = \alpha_j^{(r)} + s_j^{(r)} \rho_j^{(r)}$  with  $s_j^{(r)}$  given by (4.16).
- 5: Calculate  $\omega_j^{(r+1)} = \omega_j^s + V^n \alpha_j^{(r+1)}$ .
- 6: Update  $\mathbf{m}^{(r+1)}$  by (4.17).
- 7:  $r = r + 1$ .
- 8: **end while**

---

**5. Convergence analysis of the IRCSI and IRSOM algorithms.** The IRCSI and IRSOM algorithms can be reformulated in a unified framework. For  $x_j \in \mathbb{C}^{n_j}, y \in \mathbb{C}^m$  with integers  $m, n_j > 0$ ,  $j = 1, \dots, J$ , write  $x = (x_1, \dots, x_J)$

and define  $\Psi(x, y) = \Psi(x_1, \dots, x_J, y) := \sum_{j=1}^J \Psi_j(x_j, y)$  with  $\Psi_j(\cdot, \cdot) : \mathbb{C}^{n_j} \times \mathbb{C}^m \rightarrow \mathbb{R}$  being continuously differentiable. Now consider the following iteratively regularized CSI-type (IRCSI-type) method:

$$(5.1) \quad x_j^{k+1} = x_j^k + s_j^k v_j^k, \quad j = 1, \dots, J,$$

$$(5.2) \quad s_j^k \in \arg \min_s \Psi_j(x_j^k + sv_j^k, y^k) + \gamma \|sv_j^k\|_1,$$

$$(5.3) \quad y^{k+1} \in \arg \min_y \sum_{j=1}^J \Psi_j(x_j^{k+1}, y) + \beta \|y - y^k\|_1,$$

where the PR-CG direction  $v_j^k$  is defined by

$$(5.4) \quad v_j^k := \begin{cases} g_j^0, & k = 0, \\ g_j^k + \frac{\operatorname{Re} \langle g_j^k, g_j^k - g_j^{k-1} \rangle}{\|g_j^{k-1}\|^2} v_j^{k-1}, & k \geq 1 \text{ and } g_j^{k-1} \neq 0, \\ g_j^k, & k \geq 1 \text{ and } g_j^{k-1} = 0, \end{cases}$$

with  $g_j^k = \nabla_{x_j} \Psi_j(x_j^k, y^k)$  which is defined in the following Definition 5.1. In the rest of the paper, let  $\|\cdot\|_\infty$  denote the infinity norm of a vector or the maximum absolute row sum norm of a matrix.

**DEFINITION 5.1.** *Let  $\psi(z) : \mathbb{C}^n \rightarrow \mathbb{R}$  be a real-valued function defined on the complex domain  $\mathbb{C}^n$ . For any  $z = z_r + iz_i$  with  $z_r, z_i \in \mathbb{R}^n$ , the function  $\psi(z)$  can be equivalently represented as a real-variable function  $\tilde{\psi}(z_r, z_i)$  mapping  $\mathbb{R}^n \times \mathbb{R}^n$  to  $\mathbb{R}$ .  $\psi(z)$  is called continuously differentiable (denoted as  $\psi \in C^1$ ) if  $\tilde{\psi}(z_r, z_i)$  is continuously differentiable in  $\mathbb{R}^n \times \mathbb{R}^n$ . The complex gradient operator  $\nabla_z \psi(z)$  is defined as*

$$\nabla_z \psi(z) := \nabla_{z_r} \tilde{\psi}(z_r, z_i) + i \nabla_{z_i} \tilde{\psi}(z_r, z_i).$$

If  $y = \mathbf{m}$ ,  $x_j = \boldsymbol{\omega}_j$  and  $\Psi_j(x_j, y) = F_j^{csi}(\boldsymbol{\omega}_j, \mathbf{m})$ ,  $j = 1, \dots, J$ , then the IRCSI-type method (5.1)–(5.3) becomes the IRCSI method with the subproblems (5.2) and (5.3) having explicit solutions (4.9) and (4.10), respectively. If  $y = \mathbf{m}$ ,  $x_j = \boldsymbol{\alpha}_j$  and  $\Psi_j(x_j, y) = F_j^{som}(\boldsymbol{\alpha}_j, \mathbf{m})$ ,  $j = 1, \dots, J$ , then the IRCSI-type method (5.1)–(5.3) becomes the IRSOM method with the subproblems (5.2) and (5.3) having explicit solutions (4.16) and (4.17), respectively.

To prove the convergence of the iterative solutions  $\{(x^k, y^k)\}_{k \in \mathbb{N}}$  of the IRCSI-type method (5.1)–(5.3) with  $x^k = (x_1^k, \dots, x_J^k)$ , we need to make certain assumptions on the objective function  $\Psi(x, y) = \sum_{j=1}^J \Psi_j(x_j, y)$ .

**Assumption 5.2.** (i) For each  $j = 1, \dots, J$ ,  $\Psi_j(x_j, y) : \mathbb{C}^{n_j} \times \mathbb{C}^m \rightarrow \mathbb{R}$  is  $C^1$ , that is,  $\nabla_{x_j} \Psi_j(x_j, y)$  and  $\nabla_y \Psi_j(x_j, y)$  are both continuous.

(ii)  $\inf_{(x, y) \in \mathbb{C}^{n_1} \times \dots \times \mathbb{C}^m} \Psi(x, y) > -\infty$ .

**Remark 5.3.** It is easy to prove that  $\nabla_{\boldsymbol{\omega}_j} F_j^{csi}$ ,  $\nabla_{\mathbf{m}} F_j^{csi}$ ,  $\nabla_{\boldsymbol{\alpha}_j} F_j^{som}$  and  $\nabla_{\mathbf{m}} F_j^{som}$  are continuous for all  $j$ , so  $F_j^{csi}$  and  $F_j^{som}$  are  $C^1$  functions for all  $j$ . In addition, it is clear that  $F_j^{csi} \geq 0$  and  $F_j^{som} \geq 0$ . Thus the functions  $F_j^{csi}$ ,  $F_j^{som}$ ,  $F_j^{csi}$  and  $F_j^{som}$  satisfy Assumption 5.2.

**THEOREM 5.4.** *Suppose Assumption 5.2 holds and let  $\{z^k = (x^k, y^k)\}_{k \in \mathbb{N}}$  be the sequence generated by the IRCSI-type method (5.1)–(5.3) with  $\gamma, \beta > 0$ . Then the following statements hold:*

(i) The sequence  $\{z^k\}_{k \in \mathbb{N}}$  is convergent.  
(ii) Let  $L \geq \max_{1 \leq j \leq J} \sqrt{n_j}$  be a constant such that  $\|\xi\|_1 \leq L\|\xi\|$  for any  $\xi \in \mathbb{C}^{n_j}$ ,  $j = 1, \dots, J$  and let  $\varepsilon = \max\{\gamma L, \beta\}$ . Then the limit point  $z^*$  of  $\{z^k\}_{k \in \mathbb{N}}$  is an  $\varepsilon$ -stationary point of the objective function  $\Psi$ , that is,

$$(5.5) \quad \|\nabla \Psi(z^*)\|_\infty \leq \varepsilon.$$

*Proof.* (i) From (5.1)–(5.3) it follows that for any  $k \in \mathbb{N}$ ,

$$(5.6) \quad \gamma \|x_j^{k+1} - x_j^k\|_1 \leq \Psi_j(x_j^k, y^k) - \Psi_j(x_j^{k+1}, y^k), \quad j = 1, \dots, J,$$

$$(5.7) \quad \beta \|y^{k+1} - y^k\|_1 \leq \Psi(x^{k+1}, y^k) - \Psi(x^{k+1}, y^{k+1}).$$

Summing up (5.6) with respective to  $j$  gives

$$(5.8) \quad \gamma \|x^{k+1} - x^k\|_1 \leq \Psi(x^k, y^k) - \Psi(x^{k+1}, y^k).$$

By (5.7) and (5.8), we know  $\Psi(x^k, y^k) \geq \Psi(x^{k+1}, y^{k+1})$ . This, together with the fact that  $\inf \Psi > -\infty$ , implies that

$$(5.9) \quad \lim_{k \rightarrow \infty} \Psi(z^k) = \Psi^* \quad \text{for some } \Psi^* \in \mathbb{R}.$$

Now, summing up (5.7) and (5.8) for all  $k \in \mathbb{N}$ , we get

$$\begin{aligned} \sum_{k=0}^{\infty} [\gamma \|x^{k+1} - x^k\|_1 + \beta \|y^{k+1} - y^k\|_1] &\leq \sum_{k=0}^{\infty} [\Psi(x^k, y^k) - \Psi(x^{k+1}, y^{k+1})] \\ &\leq \Psi(z^0) - \Psi^* < +\infty, \end{aligned}$$

which means that the sequence  $\{z^k\}_{k \in \mathbb{N}}$  is a Cauchy sequence so  $\{z^k\}_{k \in \mathbb{N}}$  is convergent.

(ii) Since  $s_j^k$  is a minimum solution with respect to  $s$  of  $\Psi_j(x_j^k + sv_j^k, y^k) + \gamma \|sv_j^k\|_1$  (see (5.2)), then the partial derivative (see Definition 5.1)

$$\partial_s \Psi_j(x_j^k + sv_j^k, y^k)|_{s=s_j^k} = \langle \nabla_{x_j} \Psi_j(x_j^{k+1}, y^k), v_j^k \rangle$$

is a sub-gradient of  $-\gamma \|v_j^k\|_1 \partial|s_j^k|$ , and thus we have

$$(5.10) \quad |\langle \nabla_{x_j} \Psi_j(x_j^{k+1}, y^k), v_j^k \rangle| \leq \gamma \|v_j^k\|_1.$$

Let  $(x^*, y^*)$  be the convergent point of  $\{(x^k, y^k)\}_{k \in \mathbb{N}}$ . Since  $\Psi_j$  is a  $C^1$  function, then

$$(5.11) \quad \lim_{k \rightarrow \infty} \nabla_{x_j} \Psi_j(x_j^{k+1}, y^k) = \nabla_{x_j} \Psi_j(x_j^*, y^*) =: g_j^*, \quad \forall j = 1, \dots, J.$$

We now claim that for all  $j = 1, \dots, J$ ,

$$(5.12) \quad \|g_j^*\| \leq \gamma L.$$

In fact, suppose this were not true, that is,  $\|g_{j_0}^*\| > \gamma L$  for some  $j_0 \in \{1, \dots, J\}$ . Then there would exist a sufficiently large  $k_0$  such that  $\|g_{j_0}^{k-1}\| > \gamma L$  for all  $k > k_0$ . By (5.4) we obtain that

$$(5.13) \quad \|v_{j_0}^k - g_{j_0}^k\| \leq \frac{\|g_{j_0}^k\| \|g_{j_0}^k - g_{j_0}^{k-1}\|}{\|g_{j_0}^{k-1}\|^2} \|v_{j_0}^{k-1}\| \leq \frac{\|g_{j_0}^k\| \|g_{j_0}^k - g_{j_0}^{k-1}\|}{(\gamma L)^2} \|v_{j_0}^{k-1}\|, \quad \forall k > k_0.$$

Since  $\lim_{k \rightarrow \infty} g_j^k = g_j^*$  for  $j = 1, \dots, J$ , then there is a  $k_1 > k_0$  such that

$$\|v_{j_0}^k\| \leq \|g_{j_0}^*\| + 1 + \frac{1}{2}\|v_{j_0}^{k-1}\|, \quad \forall k > k_1.$$

This yields that  $\|v_{j_0}^k\| \leq 2\|g_{j_0}^*\| + 2 + \|v_{j_0}^{k_1}\|/2$  for all  $k > k_1$ . Thus, by letting  $k \rightarrow \infty$  in (5.13) we get

$$(5.14) \quad \lim_{k \rightarrow \infty} v_{j_0}^k = g_{j_0}^*.$$

Letting  $k \rightarrow \infty$  in (5.10) and making use of (5.11) and (5.14), we have

$$\|g_{j_0}^*\|^2 \leq \gamma\|g_{j_0}^*\|_1 \leq \gamma L\|g_{j_0}^*\|,$$

where use has been made of the assumption  $\|\xi\|_1 \leq L\|\xi\|$  for any  $\xi \in \mathbb{C}^{n_j}$ ,  $j = 1, \dots, J$ . This contradicts the condition that  $\|g_{j_0}^*\| > \gamma L$ , so the claim (5.12) is true. Thus for all  $j$ ,

$$\|g_j^*\|_\infty \leq \|g_j^*\| \leq \gamma L.$$

Since  $\|\nabla_x \Psi(x, y)\|_\infty = \max_{1 \leq j \leq J} \|\nabla_{x_j} \Psi_j(x_j, y)\|_\infty$ , then

$$(5.15) \quad \|\nabla_x \Psi(x^*, y^*)\|_\infty \leq \gamma L.$$

Similarly, by (5.3) we know that  $\nabla_y \Psi(x^{k+1}, y^{k+1})$  is a sub-gradient of  $-\beta \partial_y \|y - y^k\|_1$  at the point  $y^{k+1}$ , so

$$\|\nabla_y \Psi(x^{k+1}, y^{k+1})\|_\infty \leq \beta, \quad \forall k.$$

Letting  $k \rightarrow \infty$  in the above inequality and noting that  $\Psi_j$  is a  $C^1$  function, we get

$$(5.16) \quad \|\nabla_y \Psi(x^*, y^*)\|_\infty \leq \beta.$$

Combining (5.15) and (5.16) gives that

$$\|\nabla \Psi(z^*)\|_\infty \leq \max\{\gamma L, \beta\}.$$

The proof is thus complete.  $\square$

This theorem establishes the global convergence of the iteration sequence  $\{z^k = (x^k, y^k)\}_{k=1}^\infty$  generated by the IRCSI-type method (5.1)–(5.3) with the limit  $z^* = (x^*, y^*)$  of the sequence  $\{z^k\}_{k=1}^\infty$  satisfying  $\|\nabla \Psi(z^*)\|_\infty \leq \varepsilon$ , where  $\varepsilon = \max\{\gamma L, \beta\}$ . Such  $z^*$  is called an  $\varepsilon$ -stationary point of the objective function  $\Psi(x, y)$  (see also [23] for this definition for regularized variational image restoration problems).

In applications, the measurement data  $\mathbf{u}_j^{\infty, \delta}$  is usually noisy, so that it is actually impossible to find an exact critical point  $z^* = (x^*, y^*)$  of the objective function  $\Psi(x, y)$  (i.e.,  $\nabla \Psi(x^*, y^*) = 0$ ). In fact, in this case, it is sufficient to find an  $\varepsilon$ -stationary point of the objective function  $\Psi(x, y)$  for certain small  $\varepsilon$  depending actually on the noise level. In this sense, the global convergence result presented in Theorem 5.4 is reasonable, as demonstrated by the numerical experiments in Section 7. Further, the termination criterion can be chosen as

$$(5.17) \quad \|\nabla \Psi(x^k, y^k)\|_\infty \leq 2\varepsilon.$$

If  $y = \mathbf{m}$ ,  $x_j = \boldsymbol{\omega}_j$  and  $\Psi_j(x_j, y) = F_j^{csi}(\boldsymbol{\omega}_j, \mathbf{m})$ ,  $j = 1, \dots, J$  or if  $y = \mathbf{m}$ ,  $x_j = \boldsymbol{\alpha}_j$  and  $\Psi_j(x_j, y) = F_j^{som}(\boldsymbol{\alpha}_j, \mathbf{m})$ ,  $j = 1, \dots, J$ , then Assumption 5.2 is satisfied, as indicated by Remark 5.3. Then the following corollaries follow easily from Theorem 5.4.

COROLLARY 5.5. Let  $\{z^{(k)} = (\boldsymbol{\omega}^{(k)}, \mathbf{m}^{(k)})\}_{k \in \mathbb{N}}$  be the sequence generated by the IRCSI algorithm (Algorithm 4.1) with  $\gamma, \beta > 0$ . Then the following statements hold.

(i) The sequence  $\{z^{(k)}\}_{k \in \mathbb{N}}$  is convergent.

(ii) Let  $L \geq \max_{1 \leq j \leq J} \sqrt{n_j}$  be a constant such that  $\|\xi\|_1 \leq L\|\xi\|$  for any  $\xi \in \mathbb{C}^{n_j}$ ,  $j = 1, \dots, J$  and  $\varepsilon = \max\{\gamma L, \beta\}$ . Then the limit point  $z^*$  of  $\{z^{(k)}\}_{k \in \mathbb{N}}$  is an  $\varepsilon$ -stationary point of the objective function  $F^{csi}$ , that is,

$$\|\nabla F^{csi}(z^*)\|_\infty \leq \varepsilon.$$

COROLLARY 5.6. Let  $\{z^{(k)} = (\boldsymbol{\alpha}^{(k)}, \mathbf{m}^{(k)})\}_{k \in \mathbb{N}}$  be the sequence generated by the IRSOM algorithm (Algorithm 4.2) with  $\gamma, \beta > 0$ . Then the following statements hold.

(i) The sequence  $\{z^{(k)}\}_{k \in \mathbb{N}}$  is convergent.

(ii) Let  $L \geq \max_{1 \leq j \leq J} \sqrt{n_j}$  be a constant such that  $\|\xi\|_1 \leq L\|\xi\|$  for any  $\xi \in \mathbb{C}^{n_j}$ ,  $j = 1, \dots, J$  and  $\varepsilon = \max\{\gamma L, \beta\}$ . Then the limit point  $z^*$  of  $\{z^{(k)}\}_{k \in \mathbb{N}}$  is an  $\varepsilon$ -stationary point of the objective function  $F^{som}$ , that is,

$$\|\nabla F^{som}(z^*)\|_\infty \leq \varepsilon.$$

Corollaries 5.5 and 5.6 ensure that the iterative sequence  $\{z^{(k)} = (\boldsymbol{\omega}^{(k)}, \mathbf{m}^{(k)})\}_{k \in \mathbb{N}}$  obtained by the IRCSI algorithm (or  $\{z^{(k)} = (\boldsymbol{\alpha}^{(k)}, \mathbf{m}^{(k)})\}_{k \in \mathbb{N}}$  obtained by the IRSOM algorithm) converges globally to an  $\varepsilon$ -stationary point  $z^*$  of the objective function  $F^{csi}(z)$  with  $z = (\boldsymbol{\omega}, \mathbf{m})$  (or  $F^{som}(z)$  with  $z = (\boldsymbol{\alpha}, \mathbf{m})$ ). Rewrite  $F^{csi}((\boldsymbol{\omega}, \mathbf{m}); \mathbf{u}^{\infty, \delta})$  for  $F^{csi}(\boldsymbol{\omega}, \mathbf{m})$  defined in (3.1) and  $F^{som}((\boldsymbol{\alpha}, \mathbf{m}); \mathbf{u}^{\infty, \delta})$  for  $F^{som}(\boldsymbol{\alpha}, \mathbf{m})$  defined in (3.8) to indicate explicitly the dependence on  $\mathbf{u}^{\infty, \delta} = (\mathbf{u}_1^{\infty, \delta}, \dots, \mathbf{u}_J^{\infty, \delta})$ . Then, by Corollaries 5.5 and 5.6 we have

$$(5.18) \quad \|\nabla F^{csi}(z^*; \mathbf{u}^{\infty, \delta})\|_\infty \leq \varepsilon \quad (\text{or } \|\nabla F^{som}(z^*; \mathbf{u}^{\infty, \delta})\|_\infty \leq \varepsilon),$$

where  $\varepsilon = \max\{\gamma L, \beta\}$ , as defined in Corollary 5.5 (or Corollary 5.6).

On the other hand, let  $\mathbf{m}^\dagger$  be the ground truth solution of the discrete inverse medium scattering problem defined at the end of Section 2 and let  $\boldsymbol{\omega}^\dagger = (\boldsymbol{\omega}_1^\dagger, \dots, \boldsymbol{\omega}_J^\dagger)$  with  $\boldsymbol{\omega}_j^\dagger$  being the solution of the discrete state equation (2.10) (that is, the discrete form of the Lippmann–Schwinger integral equation (2.8)) corresponding to  $\mathbf{m}^\dagger$ . Further, let  $\boldsymbol{\alpha}^\dagger = (\boldsymbol{\alpha}_1^\dagger, \dots, \boldsymbol{\alpha}_J^\dagger) = ((V^n)^* \boldsymbol{\omega}_1^\dagger, \dots, (V^n)^* \boldsymbol{\omega}_J^\dagger)$  with  $V^n$  defined as in Section 3 and let  $\varepsilon_h = \max_{1 \leq j \leq J} \|\mathbf{u}_j^\infty - T^\infty \boldsymbol{\omega}_j^\dagger\|$ . Therefore, for noisy measurement data  $\mathbf{u}^{\infty, \delta}$ , we have that for  $z^\dagger = (\boldsymbol{\omega}^\dagger, \mathbf{m}^\dagger)$ ,

$$(5.19) \quad \begin{aligned} \|\nabla F^{csi}(z^\dagger; \mathbf{u}^{\infty, \delta})\|_\infty &= \max_{1 \leq j \leq J} \left\| 2\eta_{d,j} (T^\infty)^* (T^\infty \boldsymbol{\omega}_j^\dagger - \mathbf{u}_j^{\infty, \delta}) \right\|_\infty \\ &\leq \max_{1 \leq j \leq J} \{2\eta_{d,j}\} \|(T^\infty)^*\|_{\infty, 2} (\varepsilon_h + \delta), \end{aligned}$$

where  $\|\cdot\|_{\infty, 2}$  is defined by  $\|A\|_{\infty, 2} := \max_i (\sum_j |a_{ij}|^2)^{1/2}$  for any matrix  $A = (a_{ij})$ . Moreover, we have that for  $z^\dagger = (\boldsymbol{\alpha}^\dagger, \mathbf{m}^\dagger)$  and sufficiently small  $h > 0$ ,

$$(5.20) \quad \begin{aligned} \|\nabla F^{som}(z^\dagger; \mathbf{u}^{\infty, \delta})\|_\infty &= \max \left\{ \max_{1 \leq j \leq J} \|\nabla_{\boldsymbol{\alpha}_j} F^{som}(z^\dagger; \mathbf{u}^{\infty, \delta})\|_\infty, \|\nabla_{\mathbf{m}} F^{som}(z^\dagger; \mathbf{u}^{\infty, \delta})\|_\infty \right\} \\ &\leq C_0 \max_{1 \leq j \leq J} \left\{ 2\eta_{s,j} \|\boldsymbol{\omega}_j^s + V^n \boldsymbol{\alpha}_j^\dagger - \boldsymbol{\omega}_j^\dagger\|_\infty \right\} \\ &\quad + \max_{1 \leq j \leq J} \left\{ 2\eta_{d,j} \left\| (T^\infty V^n)^* (T^\infty (\boldsymbol{\omega}_j^s + V^n \boldsymbol{\alpha}_j^\dagger) - \mathbf{u}_j^{\infty, \delta}) \right\|_\infty \right\} \\ &\leq C \max \left[ \|\widehat{V}^s\|_{\infty, 2} \max_{1 \leq j \leq J} \{2\eta_{s,j}\}, \lambda_{L_\alpha+1} \max_{1 \leq j \leq J} \{2\eta_{d,j}\} \right] (\varepsilon_h + \delta) \end{aligned}$$

with  $\widehat{V}^s := (\mathbf{v}_1/\lambda_1, \dots, \mathbf{v}_{L_\alpha}/\lambda_{L_\alpha}) \in \mathbb{C}^{M \times L_\alpha}$  and with  $C_0$  and  $C$  being constants independent of  $h$ . Here, we use the facts that  $\limsup_{h \rightarrow +0} \|T\|_\infty < \infty$  (see [51, 52]),

$$\begin{aligned} \|\boldsymbol{\omega}_j^s + V^n \boldsymbol{\alpha}_j^\dagger - \boldsymbol{\omega}_j^\dagger\|_\infty &= \left\| \sum_{k=1}^{L_\alpha} \frac{\langle \mathbf{u}_j^{\infty, \delta} - T^\infty \boldsymbol{\omega}_j^\dagger, \mathbf{u}_k \rangle}{\lambda_k} \mathbf{v}_k \right\|_\infty \\ &\leq \|\widehat{V}^s\|_{\infty, 2} \|T^\infty \boldsymbol{\omega}_j^\dagger - \mathbf{u}_j^{\infty, \delta}\| \end{aligned}$$

and

$$\begin{aligned} &\left\| (T^\infty V^n)^* (T^\infty (\boldsymbol{\omega}_j^s + V^n \boldsymbol{\alpha}_j^\dagger) - \mathbf{u}_j^{\infty, \delta}) \right\|_\infty \\ &= \left\| (T^\infty V^n)^* \sum_{k \geq L_\alpha + 1} \langle T^\infty \boldsymbol{\omega}_j^\dagger - \mathbf{u}_j^{\infty, \delta}, \mathbf{u}_k \rangle \mathbf{u}_k \right\|_\infty \leq \lambda_{L_\alpha + 1} \|T^\infty \boldsymbol{\omega}_j^\dagger - \mathbf{u}_j^{\infty, \delta}\|. \end{aligned}$$

It is known from [51, 52] that  $\lim_{h \rightarrow +0} \varepsilon_h = 0$ . Therefore, for sufficiently small  $h > 0$ , the  $z^\dagger$  satisfying (5.19) (resp. (5.20)) can be called the  $O(\delta^{csi})$ -stationary point of the objective function  $F^{csi}(z; \mathbf{u}^{\infty, \delta})$  (resp. the  $O(\delta^{som})$ -stationary point of the objective function  $F^{som}(z; \mathbf{u}^{\infty, \delta})$ ), where  $\delta^{csi}$  and  $\delta^{som}$  are given by

$$(5.21) \quad \begin{cases} \delta^{csi} := \|(T^\infty)^*\|_{\infty, 2} \max_{1 \leq j \leq J} \{2\eta_{d,j}\} \delta, \\ \delta^{som} := \max \left[ \|\widehat{V}^s\|_{\infty, 2} \max_{1 \leq j \leq J} \{2\eta_{s,j}\}, \lambda_{L_\alpha + 1} \max_{1 \leq j \leq J} \{2\eta_{d,j}\} \right] \delta. \end{cases}$$

From (5.18), (5.19) and (5.20), we know that in the noisy data case, for sufficiently small  $h > 0$ , it is better to choose the regularization parameters  $\gamma$  and  $\beta$  such that

$$(5.22) \quad \begin{aligned} &\max\{\gamma L, \beta\} = O(\delta^{csi}) \quad \text{for the IRCSI algorithm} \\ &\text{(or } \max\{\gamma L, \beta\} = O(\delta^{som}) \text{ for the IRSOM algorithm).} \end{aligned}$$

**6. Numerical experiments.** This section presents two numerical examples to evaluate the performance of Algorithms 4.1 and 4.2. For the objective function  $F^{csi}$  in (3.1), we set

$$\eta_{s,j} = \left( \sum_{j=1}^J \|\mathbf{m}^{(0)} \odot \mathbf{u}_j^i\|^2 \right)^{-1} \quad \text{and} \quad \eta_{d,j} = \left( \sum_{j=1}^J \|\mathbf{u}_j^{\infty, \delta}\|^2 \right)^{-1}, \quad j = 1, \dots, J,$$

which are positive constants. Then the original CSI method (3.3)–(3.5) is just Algorithm 4.1 with  $\gamma = \beta = 0$ . For the objective function  $F^{som}$  in (3.8), we set  $\eta_{s,j}$  and  $\eta_{d,j}$  as in [15] and choose  $L_\alpha = 10$ . Then the original SOM method (3.10)–(3.12) is just Algorithm 4.2 with  $\gamma = \beta = 0$ .

We only consider the two-dimensional case in the numerical examples. In all the numerical examples, we choose the scatterers located in the region  $[-2, 2] \times [-2, 2]$ . For the synthetic far-field data, we discretize the above region into  $256 \times 256$  small boxes using the method presented in Section 2. To avoid the inverse crime, we discretize the same region into  $64 \times 64$  small boxes via the same method in each iteration of our algorithms. Furthermore, we choose  $\gamma = \beta/64$  and  $L = 64$  so that  $\gamma L = \beta$  always holds. Then  $\varepsilon = \beta$  (see Theorem 5.4) is the only varying parameter for different IRCSI-type algorithms. We will compare the performance of five

IRCSI algorithms (with  $\beta = 0, 10^{-6}, 10^{-5}, 10^{-4}$  and  $10^{-3}$ ) and five IRSOM algorithms (with  $\beta = 0, 10^{-5}, 10^{-4}, 10^{-3}$  and  $10^{-2}$ ). To study the convergence property of these IRCSI-type algorithms, we allow these algorithms to run a sufficiently large number of iterations without using the termination criterion (5.17). In addition, in order to quantitatively evaluate the reconstruction results, we calculate the relative errors (RE) at all iterations for each example. The relative error of the reconstruction result  $y^k$  at the  $k$ -th iteration of the contrast is defined as

$$R^k := \frac{\|y^k - y^\dagger\|_F}{\|y^\dagger\|_F},$$

where  $y^\dagger$  is the ground truth contrast and  $\|\cdot\|_F$  is the Frobenius norm. We consider both noiseless and noisy measurement data. For the noisy case, the measurement data  $\mathbf{u}_j^{\infty, \delta}$  are obtained by adding 5% relative noise to the exact far-field data  $\mathbf{u}_j^\infty$ , that is,

$$\frac{\|\mathbf{u}_j^{\infty, \delta} - \mathbf{u}_j^\infty\|}{\|\mathbf{u}_j^\infty\|} \leq 5\%, \quad j = 1, \dots, J.$$

This means that  $\mathbf{u}_j^{\infty, \delta}$  ( $j = 1, \dots, J$ ) satisfy (2.14) with

$$(6.1) \quad \delta = 0.05 \max_{1 \leq j \leq J} \|\mathbf{u}_j^\infty\| \approx 0.05 \max_{1 \leq j \leq J} \|\mathbf{u}_j^{\infty, \delta}\|.$$

In the first example, we consider a scatterer whose contrast  $m(x)$  is  $e^{-1/(1-|x|^2)}$  for  $|x| < 1$  and zero elsewhere. The wave number  $k = 6$  and  $J = Q = 16$ . We choose  $d_j = (\cos(2\pi(j-1)/J), \sin(2\pi(j-1)/J))$  ( $j = 1, \dots, J$ ) and  $\hat{x}^q = (\cos(2\pi(q-1)/Q), \sin(2\pi(q-1)/Q))$  ( $q = 1, \dots, Q$ ), which are 16 incident and 16 measurement directions uniformly distributed on the unit circle. Fig. 1 and Fig. 2 present the ground truth and the reconstruction results of the IRCSI algorithm with  $\beta = 0, 10^{-6}, 10^{-5}, 10^{-4}, 10^{-3}$  and the IRSOM algorithm with  $\beta = 0, 10^{-5}, 10^{-4}, 10^{-3}, 10^{-2}$  both at the 30000-th iteration from the noisy data with 5% noise and at the 5000-th iteration from the noiseless data, respectively. The top row in Fig. 1 and Fig. 2 shows the ground truth and the reconstruction results of the IRCSI algorithm, whilst the bottom row in Fig. 1 and Fig. 2 shows the reconstruction results of the IRSOM algorithm. Fig. 3 and Fig. 4 present the relative error (RE)  $R^k$  of the reconstruction result  $y^k$  at the  $k$ -th iteration against the iteration step  $k$  in the cases of noisy and noiseless data, respectively.

In the second example, we consider a scatterer for which the shape of the support of its contrast  $m(x)$  is the handwritten digit 0 from the MNIST dataset [22]. The handwritten digit 0 is a grayscale image, where the grayscale value of each pixel ranges from an integer in  $[0, 255]$ , and the contrast value of the scatterer, ranging from 0 to 1, is obtained by dividing the grayscale value by 255. The other settings and the parameters of this example are the same as in the first example. Fig. 5 and Fig. 6 present the ground truth and the reconstruction results of the IRCSI algorithm with  $\beta = 0, 10^{-6}, 10^{-5}, 10^{-4}, 10^{-3}$  and the IRSOM algorithm with  $\beta = 0, 10^{-5}, 10^{-4}, 10^{-3}, 10^{-2}$  both at the 50000-th iteration from the noisy data with 5% noise and at the 10000-th iteration from the noiseless data, respectively. The top row in Fig. 5 and Fig. 6 shows the ground truth and the reconstruction results of the IRCSI algorithm, whilst the bottom row in Fig. 5 and Fig. 6 gives the reconstruction results of the IRSOM algorithm. Fig. 7 and Fig. 8 show the relative error (RE)  $R^k$

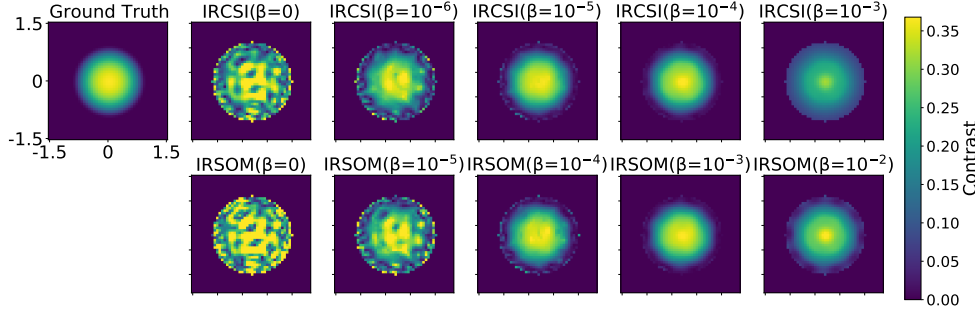


FIG. 1. The ground truth  $m(x) = e^{-1/(1-|x|^2)}$  and the reconstruction results by the IRCSI and IRSOM algorithms with different values of  $\beta$  at the 30000-th iteration from the noisy measurement data with 5% noise. Top row from left to right: the ground truth and the reconstructions by the IRCSI algorithm with  $\beta = 0, 10^{-6}, 10^{-5}, 10^{-4}, 10^{-3}$ . Bottom row from left to right: the reconstructions by the IRSOM algorithm with  $\beta = 0, 10^{-5}, 10^{-4}, 10^{-3}, 10^{-2}$ .

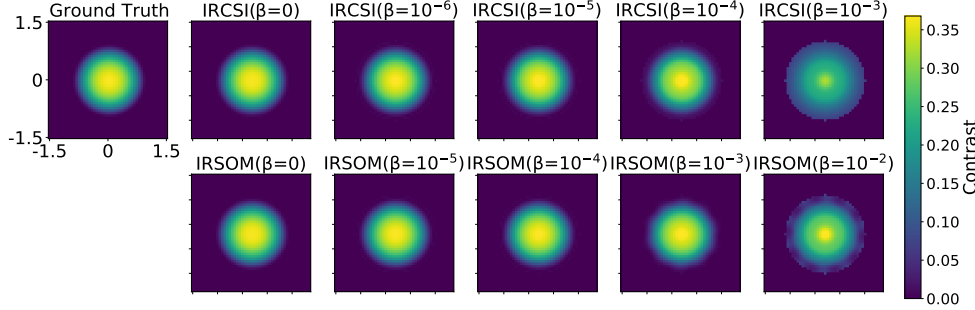


FIG. 2. The ground truth  $m(x) = e^{-1/(1-|x|^2)}$  and the reconstruction results by the IRCSI and IRSOM algorithms with different values of  $\beta$  at the 5000-th iteration from the noiseless measurement data. Top row from left to right: the ground truth and the reconstructions by the IRCSI algorithm with  $\beta = 0, 10^{-6}, 10^{-5}, 10^{-4}, 10^{-3}$ . Bottom row from left to right: the reconstructions by the IRSOM algorithm with  $\beta = 0, 10^{-5}, 10^{-4}, 10^{-3}, 10^{-2}$ .

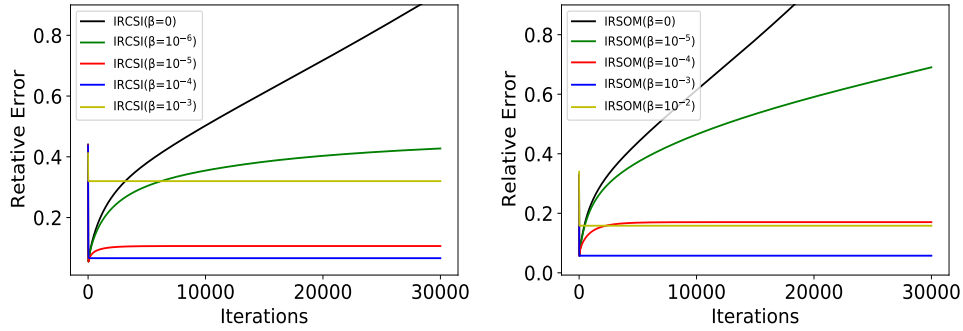


FIG. 3. The relative error between the ground truth and the reconstruction results by the IRCSI algorithm with  $\beta = 0, 10^{-6}, 10^{-5}, 10^{-4}, 10^{-3}$  (left figure) and the IRSOM algorithm with  $\beta = 0, 10^{-5}, 10^{-4}, 10^{-3}, 10^{-2}$  (right figure) against the iteration step, where the ground truth contrast is  $m(x) = e^{-1/(1-|x|^2)}$  and the relative noise of the measurement data is 5%.

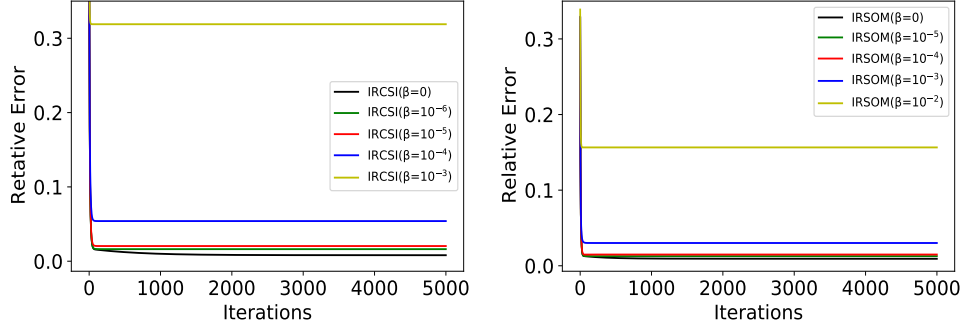


FIG. 4. The relative error between the ground truth and the reconstruction results by the IRCSI algorithm with  $\beta = 0, 10^{-6}, 10^{-5}, 10^{-4}, 10^{-3}$  (left figure) and the IRSOM algorithm with  $\beta = 0, 10^{-5}, 10^{-4}, 10^{-3}, 10^{-2}$  (right figure) against the iteration step, where the ground truth contrast is  $m(x) = e^{-1/(1-|x|^2)}$  and the measurement data has no noise.

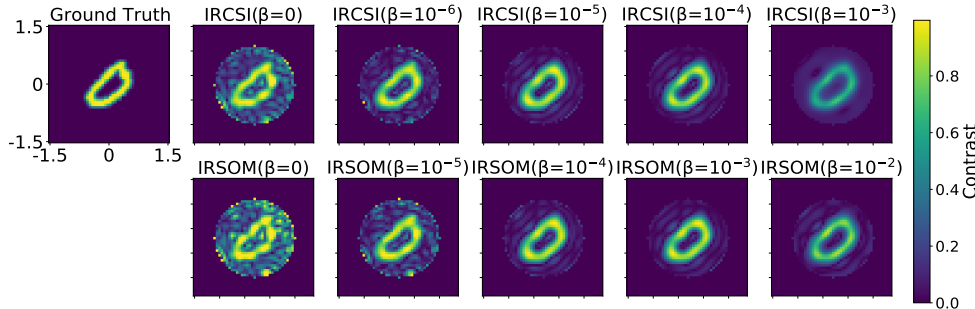


FIG. 5. The ground truth of the handwritten digit 0 image and the reconstructions by the IRCSI and IRSOM algorithms with different values of  $\beta$  at the 50000-th iteration from the noisy data with 5% noise. Top row from left to right: the ground truth and the reconstructions by the IRCSI algorithm with  $\beta = 0, 10^{-6}, 10^{-5}, 10^{-4}, 10^{-3}$ . Bottom row from left to right: the reconstructions by the IRSOM algorithm with  $\beta = 0, 10^{-5}, 10^{-4}, 10^{-3}, 10^{-2}$ .

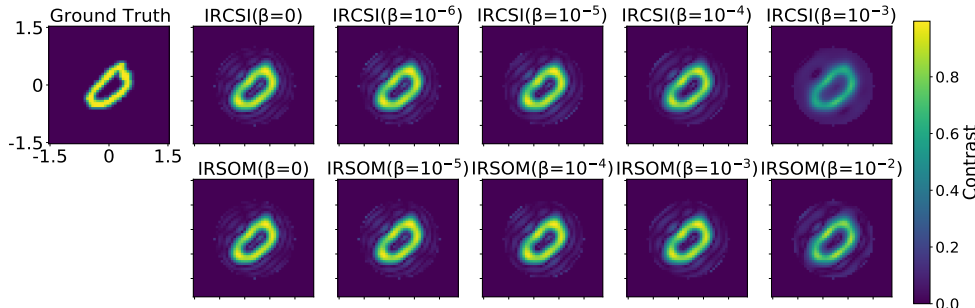


FIG. 6. The ground truth of the handwritten digit 0 image and the reconstructions by the IRCSI and IRSOM algorithms with different values of  $\beta$  at the 10000-th iteration from the noiseless data. Top row from left to right: the ground truth and the reconstructions by the IRCSI algorithm with  $\beta = 0, 10^{-6}, 10^{-5}, 10^{-4}, 10^{-3}$ . Bottom row from left to right: the reconstructions by the IRSOM algorithm with  $\beta = 0, 10^{-5}, 10^{-4}, 10^{-3}, 10^{-2}$ .

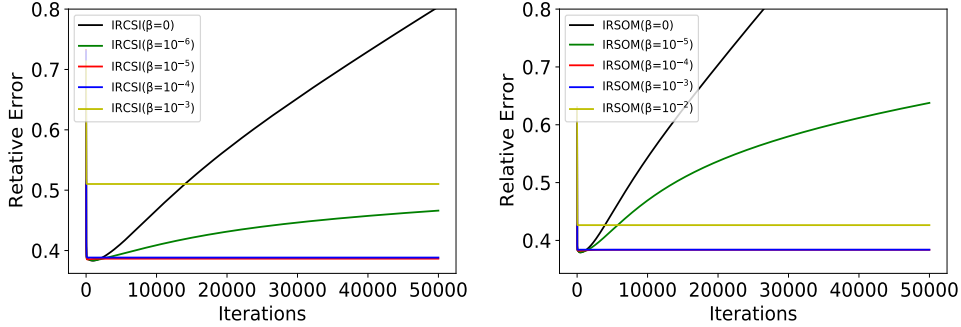


FIG. 7. The relative error between the ground truth and the reconstruction results by the IRCSI algorithm with  $\beta = 0, 10^{-6}, 10^{-5}, 10^{-4}, 10^{-3}$  (left figure) and the IRSOM algorithm with  $\beta = 0, 10^{-5}, 10^{-4}, 10^{-3}, 10^{-2}$  (right figure) against the iteration step for the handwritten digit 0 image case, where the relative noise of the measurement data is 5%.

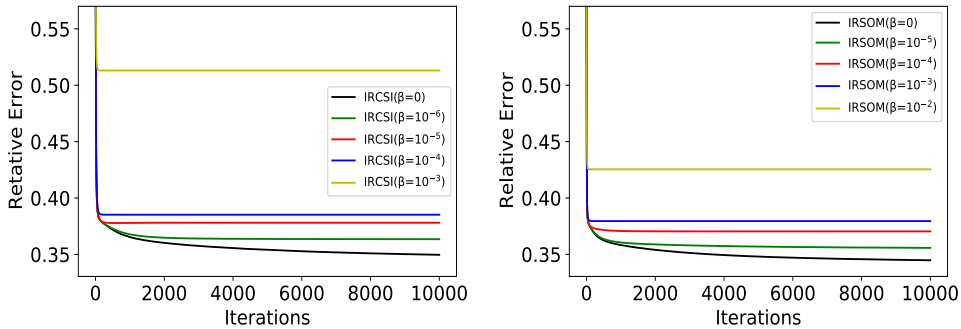


FIG. 8. The relative error between the ground truth and the reconstruction results by the IRCSI algorithm with  $\beta = 0, 10^{-6}, 10^{-5}, 10^{-4}, 10^{-3}$  (left figure) and the IRSOM algorithm with  $\beta = 0, 10^{-5}, 10^{-4}, 10^{-3}, 10^{-2}$  (right figure) against the iteration step in the handwritten digit 0 image case with noiseless data.

of the reconstruction result  $y^k$  at the  $k$ -th iteration against the iteration step  $k$  in the cases of noisy and noiseless data, respectively.

From the numerical results presented above we have the following observations.

1) In the noiseless data case, the original CSI and SOM algorithms (that is, the IRCSI and IRSOM algorithms with  $\beta = 0$ , respectively) and the IRCSI and IRSOM algorithms with small  $\beta > 0$  can give satisfactory reconstructions (see Fig. 2 and Fig. 6 for the IRCSI algorithm with  $\beta = 10^{-6}, 10^{-5}, 10^{-4}$  and for the IRSOM algorithm with  $\beta = 10^{-5}, 10^{-4}, 10^{-3}$ ). Moreover, from the relative error of the reconstruction result at each iteration (see Fig. 4 and Fig. 8) it is found that the original CSI and SOM algorithms are convergent in the noiseless data case.

2) In the noisy data case (see Fig. 3 and Fig. 7), it seems that the original CSI and SOM algorithms may not be convergent since the relative error obtained by them is still increasing after 30000 iterations in the first example (see Fig. 3) or after 50000 iterations in the second example (see Fig. 7). However, the IRCSI and IRSOM algorithms with  $\beta > 0$  are all convergent in this case, as confirmed by the theoretical convergence results presented in Corollaries 5.5 and 5.6. In particular, from Fig. 3, Fig. 7 and the numerical experiments conducted but not presented here,

it can be seen that for both two examples, the IRCSI algorithm with  $\beta = 10^{-6}$  and the IRSOM algorithm with  $\beta = 10^{-5}$  converge very slowly, but they all eventually converge after 400000 iterations. Furthermore, Fig. 1, Fig. 3, Fig. 5 and Fig. 7 show that the reconstruction results obtained by the original CSI and SOM algorithms are much worse than those obtained by the IRCSI and IRSOM algorithms with  $\beta > 0$  in the noisy data case. In the noisy data case, the ground truth solution is a  $O(\delta^{csi})$ -stationary point of  $F^{csi}(z; \mathbf{u}^{\infty, \delta})$  or a  $O(\delta^{som})$ -stationary point of  $F^{som}(z; \mathbf{u}^{\infty, \delta})$  (see (5.19), (5.20) and (5.21)), but the limit point  $z^*$  of the iterative sequence obtained by the IRCSI and IRSOM algorithms is a  $\beta$ -stationary point of the objective function  $F^{csi}(z; \mathbf{u}^{\infty, \delta})$  or  $F^{som}(z; \mathbf{u}^{\infty, \delta})$  (see (5.18)) (noting that  $\varepsilon = \beta$  here). Thus, if  $\beta$  is much smaller than  $\delta^{csi}$  for the IRCSI algorithm (or  $\delta^{som}$  for the IRSOM algorithm), then the limit point  $z^*$  would be very different from the ground truth solution, as confirmed by Fig. 1, Fig. 3, Fig. 5 and Fig. 7. Moreover, it can also be observed from the four above figures that the IRCSI algorithm with  $\beta = 10^{-4}$  and the IRSOM algorithm with  $\beta = 10^{-3}$  provide satisfactory reconstruction results. This is indeed consistent with the selection strategy of  $\beta$  given in (5.22), since we can use (5.21), (6.1) and the measurement data  $\mathbf{u}_j^{\infty, \delta}$  to calculate that

$$\begin{aligned}\delta^{csi} &\approx 1.610 \times 10^{-4} \text{ and } \delta^{som} \approx 8.607 \times 10^{-3} \text{ in Example 1,} \\ \delta^{csi} &\approx 1.365 \times 10^{-4} \text{ and } \delta^{som} \approx 9.440 \times 10^{-3} \text{ in Example 2.}\end{aligned}$$

**7. Conclusion.** In this paper, we proposed two iteratively regularized CSI-type methods with a novel  $\ell_1$  proximal term as the iteratively regularized term, the IRCSI and IRSOM algorithms, for solving inverse medium scattering problems with a fixed frequency. The IRCSI and IRSOM algorithms have a similar computational complexity to the original CSI and SOM algorithms, respectively, and in the case when the regularization parameters  $\gamma = \beta = 0$ , they reduce to the latter, respectively. It was proved rigorously that the IRCSI and IRSOM algorithms are globally convergent under natural and weak conditions on the original objective function (see Corollaries 5.5 and 5.6). As far as we know, this is the first convergence result for iterative methods of solving nonlinear inverse scattering problems with a fixed frequency. Numerical results are presented to demonstrate the theoretical convergence of the IRCSI and IRSOM algorithms as well as their much better performance in comparison with the original CSI and SOM algorithms, especially in the noisy data case. It was also proved in the noisy data case that for sufficiently small  $h > 0$ , the ground truth solution is a  $O(\delta^{csi})$ -stationary point of  $F^{csi}(z; \mathbf{u}^{\infty, \delta})$  or a  $O(\delta^{som})$ -stationary point of  $F^{som}(z; \mathbf{u}^{\infty, \delta})$  (see (5.19), (5.20) and (5.21)), whilst the limit point  $z^*$  of the iterative sequence obtained by the IRCSI and IRSOM algorithms is an  $\varepsilon$ -stationary point of the objective function  $F^{csi}(z; \mathbf{u}^{\infty, \delta})$  or  $F^{som}(z; \mathbf{u}^{\infty, \delta})$  (see (5.18)). This suggested that in the noisy data case, it is better to choose the regularization parameters  $\gamma$  and  $\beta$  in the IRCSI and IRSOM algorithms according to the selection strategy given in (5.22), which was also confirmed by the numerical results.

**Acknowledgments.** This work was partially supported by the National Key R&D Program of China (2024YFA1012303), the NNSF of China (12431016, 12271515) and Youth Innovation Promotion Association CAS.

- [1] H. ATTOUCH, J. BOLTE, P. REDONT, AND A. SOUBEYRAN, *Proximal alternating minimization and projection methods for nonconvex problems: An approach based on the Kurdyka-Łojasiewicz inequality*, Mathematics of Operations Research, 35 (2010), pp. 438–457.
- [2] A. B. BAKUSHINSKII, *The problem of the convergence of the iteratively regularized Gauss-Newton method*, Computational Mathematics and Mathematical Physics, 32 (1992), pp. 1353–1359.
- [3] G. BAO AND P. LI, *Inverse medium scattering for three-dimensional time harmonic Maxwell equations*, Inverse Problems, 20 (2004), pp. L1–L7.
- [4] G. BAO AND P. LI, *Inverse medium scattering problems for electromagnetic waves*, SIAM Journal on Applied Mathematics, 65 (2005), pp. 2049–2066.
- [5] G. BAO AND P. LI, *Inverse medium scattering for the Helmholtz equation at fixed frequency*, Inverse Problems, 21 (2005), pp. 1621–1641.
- [6] G. BAO AND P. LI, *Numerical solution of an inverse medium scattering problem for Maxwell's equations at fixed frequency*, Journal of Computational Physics, 228 (2009), pp. 4638–4648.
- [7] G. BAO AND J. LIU, *Numerical solution of inverse scattering problems with multi-experimental limited aperture data*, SIAM Journal on Scientific Computing, 25(3) (2003), pp. 1102–1117.
- [8] G. BAO, P. LI, J. LIN AND F. TRIKI, *Inverse scattering problems with multifrequencies*, Inverse Problems, 31 (2015) 093001 (21pp).
- [9] G. BAO AND F. TRIKI, *Error estimates for the recursive linearization of inverse medium problems*, Journal of Computational Mathematics, 28 (2010), pp. 725–744.
- [10] B. BLASCHKE, A. NEUBAUER, AND O. SCHERZER, *On convergence rates for the iteratively regularized Gauss-Newton method*, IMA Journal of Numerical Analysis, 17 (1997), pp. 421–436.
- [11] J. BOLTE, S. SABACH, AND M. TEBOULLE, *Proximal alternating linearized minimization for nonconvex and nonsmooth problems*, Math. Program., 146 (2014), pp. 459–494.
- [12] M. BURGER, B. KALTENBACHER, AND A. NEUBAUER, *Iterative solution methods*, in: Handbook of Mathematical Methods in Imaging (ed. O Scherzer), Springer, 2015, pp. 431–470.
- [13] H. CHANG, S. MARCHEZINI, Y. LOU, AND T. ZENG, *Variational phase retrieval with globally convergent preconditioned proximal algorithm*, SIAM Journal on Imaging Sciences, 11 (2018), pp. 56–93.
- [14] X. CHEN, *Application of signal-subspace and optimization methods in reconstructing extended scatterers*, Journal of Optical Society of America A, 26(4) (2009), pp. 1022–1026.
- [15] X. CHEN, *Subspace-based optimization method for inverse scattering problems with an inhomogeneous background medium*, Inverse Problems, 26 (2010) 074007 (13pp).
- [16] X. CHEN, *Subspace-based optimization method for solving inverse scattering problems*, IEEE Transactions on Geoscience and Remote Sensing, 48(1) (2010), pp. 42–49.
- [17] X. CHEN, *Computational Methods for Electromagnetic Inverse Scattering*, John Wiley, 2018.
- [18] Y. CHEN, *Inverse scattering via Heisenberg's uncertainty principle*, Inverse Problems, 13 (1997), pp. 253–282.
- [19] W. CHEW AND Y. WANG, *Reconstruction of two-dimensional permittivity distribution using the distorted Born iterative method*, IEEE Transactions on Medical Imaging, 9 (1990), pp. 218–225.
- [20] D. COLTON AND R. KRESS, *Looking back on inverse scattering theory*, SIAM Review, 60 (2018), pp. 779–807.
- [21] D. COLTON AND R. KRESS, *Inverse Acoustic and Electromagnetic Scattering Theory*, 4th edn, Springer, 2019.
- [22] L. DENG, *The MNIST database of handwritten digit images for machine learning research*, IEEE Signal Processing Magazine, 29 (2012), pp. 141–142.
- [23] Y. GAO AND C. WU, *On a general smoothly truncated regularization for variational piecewise constant image restoration: construction and convergent algorithms*, Inverse Problems, 36 (2020), 045007 (33pp).
- [24] M. HANKE, *A regularizing Levenberg-Marquardt scheme, with applications to inverse groundwater filtration problems*, Inverse Problems, 13 (1997), pp. 79–95.
- [25] M. HANKE, *Regularizing properties of a truncated Newton-CG algorithm for nonlinear inverse problems*, Numerical Functional Analysis and Optimization, 18 (1997), pp. 971–993.
- [26] M. HANKE, A. NEUBAUER, AND O. SCHERZER, *A convergence analysis of the Landweber iteration for nonlinear ill-posed problems*, Numer. Math., 72 (1995), pp. 21–37.
- [27] F. HETTLICH, *The Landweber iteration applied to inverse conductive scattering problems*, Inverse Problems, 14 (1998), pp. 931–947.
- [28] T. HOHAGE, *On the numerical solution of a three-dimensional inverse medium scattering problem*, Inverse Problems, 17 (2001), pp. 1743–1763.
- [29] T. HOHAGE, *Fast numerical solution of the electromagnetic medium scattering problem and applications to the inverse problem*, Journal of Computational Physics, 214 (2006), pp. 224–

238.

- [30] T. HOHAGE AND S. LANGER, *Acceleration techniques for regularized Newton methods applied to electromagnetic inverse medium scattering problems*, Inverse Problems, 26 (2010), 074011 (15pp).
- [31] T. HOHAGE, *Logarithmic convergence rates of the iteratively regularized Gauss–Newton method for an inverse potential and an inverse scattering problem*, Inverse Problems, 13 (1997), pp. 1279–1299.
- [32] T. HOHAGE, *Convergence rates of a regularized Newton method in sound-hard inverse scattering*, SIAM Journal on Numerical Analysis, 36 (1998), pp. 125–142.
- [33] T. HOHAGE AND C. SCHORMANN, *A Newton-type method for a transmission problem in inverse scattering*, Inverse Problems, 14 (1998), pp. 1207–1227.
- [34] T. HOHAGE AND F. WEIDLING, *Verification of a variational source condition for acoustic inverse medium scattering problems*, Inverse Problems, 31 (2015), 075006 (14pp).
- [35] T. HOHAGE AND F. WEIDLING, *Variational source conditions and stability estimates for inverse electromagnetic medium scattering problems*, Inverse Probl. Imaging, 11 (2017), pp. 203–220.
- [36] B. KALTENBACHER AND B. HOFMANN, *Convergence rates for the iteratively regularized Gauss–Newton method in Banach spaces*, Inverse Problems, 26 (2010), 035007 (21pp).
- [37] B. KALTENBACHER, A. NEUBAUER, AND O. SCHERZER, *Iterative Regularization Methods for Nonlinear Ill-Posed Problems*, De Gruyter, 2008.
- [38] S. LANGER, *Investigation of preconditioning techniques for the iteratively regularized Gauss–Newton method for exponentially ill-posed problems*, SIAM Journal on Scientific Computing, 32(5) (2010), pp. 2543–2559.
- [39] S. LANGER AND T. HOHAGE, *Convergence analysis of an inexact iteratively regularized Gauss–Newton method under general source conditions*, J. Inverse Ill-Posed Probl., 15 (2007), pp. 311–327.
- [40] L. LI, H. ZHENG, AND F. LI, *Two-dimensional contrast source inversion method with phaseless data: TM case*, IEEE Transactions on Geoscience and Remote Sensing, 47 (2009), pp. 1719–1736.
- [41] K. LI, B. ZHANG AND H. ZHANG, *Reconstruction of inhomogeneous media by an iteration algorithm with a learned projector*, Inverse Problems, 40 (2024), 075008 (27pp).
- [42] Y. LIU, H. ZHAO, R. SONG, X. CHEN, C. LI, AND X. CHEN, *SOM-net: Unrolling the subspace-based optimization for solving full-wave inverse scattering problems*, IEEE Transactions on Geoscience and Remote Sensing, 60 (2022), pp. 1–15.
- [43] L. PAN, Y. ZHONG, X. CHEN, AND S. P. YEO, *Subspace-based optimization method for inverse scattering problems utilizing phaseless data*, IEEE Transactions on Geoscience and Remote Sensing, 49 (2011), pp. 981–987.
- [44] R. F. REMIS AND P. M. VAN DEN BERG, *On the equivalence of the Newton–Kantorovich and distorted Born methods*, Inverse Problems, 16 (2000), pp. L1–L4.
- [45] A. ROGER, *Newton–Kantorovich algorithm applied to an electromagnetic inverse problem*, IEEE Transactions on Antennas and Propagation, 29 (1981), pp. 232–238.
- [46] M. SALUCCI, L. POLI, F. ZARDI, L. TOSI, S. LUSA, AND A. MASSA, *Contrast source inversion of sparse targets through multi-resolution Bayesian compressive sensing*, Inverse Problems, 40 (2024), 055016 (24pp).
- [47] M. SINI, AND N.T. THANH, *Inverse acoustic obstacle scattering problems using multifrequency measurements*, Inverse Problems and Imaging, 6 (2012), pp. 749–773.
- [48] M. SINI, AND N.T. THANH, *Regularized recursive Newton-type methods for inverse scattering problems using multifrequency measurement*, ESAIM: Mathematical Modelling and Numerical Analysis, 49 (2015), pp. 459–480.
- [49] S. SUN, B. J. KOOIJ, T. JIN, AND A. G. YAROVOY, *Cross-correlated contrast source inversion*, IEEE Transactions on Antennas and Propagation, 65 (2017), pp. 2592–2603.
- [50] P. TSENG, *Convergence of a block coordinate descent method for nondifferentiable minimization*, J. Optim. Theory Appl., 109 (2001), pp. 475–494.
- [51] G. VAINIKKO, *Multidimensional weakly singular integral equations*, Springer-Verlag, Berlin, 1993.
- [52] G. VAINIKKO, *Fast solvers of the Lippmann–Schwinger equation*, in: Direct and Inverse Problems of Mathematical Physics (ed. R.P. Gilbert, J. Kajiwara and Y. Xu), Springer, 2000, pp. 423–440.
- [53] P. M. VAN DEN BERG AND R. E. KLEINMAN, *A contrast source inversion method*, Inverse Problems, 13 (1997), pp. 1607–1620.
- [54] P. M. VAN DEN BERG, A. L. VAN BROEKHOVEN, AND A. ABUBAKAR, *Extended contrast source inversion*, Inverse Problems, 15 (1999), pp. 1325–1344.

- [55] P. M. VAN DEN BERG AND A. ABUBAKAR, *Contrast source inversion method: State of art*, Progress in Electromagnetics Research, 34 (2001), pp. 189–218.
- [56] P. M. VAN DEN BERG, *Forward and Inverse Scattering Algorithms Based on Contrast Source Integral Equations*, John Wiley, 2021.
- [57] M. WANG, S. SUN, D. DAI, Y. ZHANG, AND Y. SU, *Cross-correlated subspace-based optimization method for solving electromagnetic inverse scattering problems*, IEEE Transactions on Antennas and Propagation, 72 (2024), pp. 8575–8589.
- [58] Y. M. WANG AND W. C. CHEW, *An iterative solution of the two-dimensional electromagnetic inverse scattering problem*, International Journal of Imaging Systems and Technology, 1 (1989), pp. 100–108.
- [59] X. YE AND X. CHEN, *Subspace-based distorted-Born iterative method for solving inverse scattering problems*, IEEE Transactions on Antennas and Propagation, 65 (2017), pp. 7224–7232.
- [60] R. ZHANG AND B. ZHANG, *Near-field imaging of periodic inhomogeneous media*, Inverse Problems, 30 (2014) 045004 (23pp).
- [61] M. ZHONG AND J. LIU, *On the reconstruction of media inhomogeneity by inverse wave scattering model*, Science China Mathematics, 60(10) (2017), pp. 1825–1836.
- [62] Y. ZHONG AND X. CHEN, *Twofold subspace-based optimization method for solving inverse scattering problems*, Inverse Problems, 25 (2009), 085003 (11pp).